School of Pharmacy and Biomedical Sciences

Does PITP dependant PtdIns-4-P production promote encystation in Giardia duodenalis?

Aleesha Jayne Davis
0000-0002-4278-2085

This thesis is presented for the Degree of
Master of Research (Biomedical Science)
of
Curtin University

December 2020

Declaration

To the best of my knowledge and belief this thesis contains no material previously published by any other person except where due acknowledgment has been made.

This thesis contains no material which has been accepted for the award of any other degree or diploma in any university.

Signature: [redacted]……..

Date: 19th October 2020……..

Acknowledgments

Firstly, I would like to thank my supervisors Dr Carl Mousley and Dr Rob Steuart for their constant support and mentorship over the years, from my Summer Scholarship project through to honours and masters, and sharing your passions for all things cell biology, biochemistry and parasitology.

I would like to acknowledge Kelsi Wells for constructing the expression vectors utilised in this project and Connor Lamming for the gene expression data he obtained during his honours year in the lab. Without their input, this project would not be possible.

I formally thank Curtin Health Innovation Research Institute and School of Pharmacy and Biomedical Sciences for providing the facilities to undertake my research in addition to the Australian Government Research Training Program (RTP) scholarship for supporting this research.

To all the members of Lab 140, thank you for your assistance in the lab, the Tav lunches and the endless coffees. Your friendships made each day an enjoyable one.

Thank you to all of my family and friends for their continued support and last but no means least, to my partner Noah for your constant support and putting up with my never-ending studies.

Abstract

Giardia duodenalis is an intestinal parasite with an estimated 280 million symptomatic cases annually worldwide. *Giardia* has a simple two step life-cycle: the trophozoite and the environmentally resistant cyst. The cyst is produced through the process of encystation. This process involves the production, synthesis, and secretion of cyst wall proteins (CWPs) forming an extracellular matrix, conferring environmental resistance to the cyst. The trafficking of these CWPs via encystation specific vesicles (ESVs) is the only known regulated export pathway in *G. duodenalis*. Whilst *G. duodenalis* has no known Golgi apparatus, ESVs are considered to perform a similar function. Whole cell proteomic analysis has identified the expression of a putative phosphatidylinositol transfer protein (PITP) to be elevated during encystation, however not much is known about PITP function in *G. duodenalis*, through studies in other Eukaryotes indicated that this expression profile is not coincidental. It is hypothesised that *Gd* PITP dependent PtdIns-4-P production is essential to promote trafficking of CWPs to the cell periphery during the developmental progression from the trophozoite to the environmentally resistant cyst. Preliminary data from our lab determined the increased gene expression of *Gd* PITP during encystation. In this study, a yeast heterologous expression system for PITP and *Gd* PITP was generated. *Gd* PITP was found to be toxic to numerous yeast mutants defective in PtdIns-4-P synthesis. These phenotypes are reminiscent of that determined for a unique PITP (Sfh3), suggesting that *Gd* PITP may intersect with sterol signalling. In this study, an *in vitro* assay system was also developed to determine the lipid binding activity of *Gd* PITP, to further investigate the function of this protein. As little is known about the molecular mechanisms that control encystation in *G. duodenalis*, understanding these mechanisms may act as a potential target for pharmaceutical intervention, diminishing the ability of *G. duodenalis* to successfully complete encystation, therefore ablating environmental resistance.

Table of Contents

Chapter 1

General Introduction

1.1 Epidemiology of *Giardia duodenalis*

Infective to both humans and invertebrates, *Giardia* sp. is an intestinal protozoan parasite belonging to the earliest branch of eukaryotes [1, 2]. Although it is one of the earliest eukaryotes to date, it is receiving increased interest due to its common cause of gastrointestinal illness worldwide. *Giardia duodenalis* (syn. *lamblia, intestinalis)*, is one of six species identified of *Giardia* to date and is the only species able to infect humans and is estimated to cause ~280 million symptomatic infections (giardiasis) annually worldwide [1, 3-6]. Spread primarily though the faecal-oral route, the *G. duodenalis* cyst, secreted in faeces, is responsible for the spread of infection. This is due to the environmentally resistant nature of the cyst that allows it to survive in the environment, dormant for weeks to months. Once the cyst is ingested by a host, it starts to undergoes a process known as excystation, where the cyst wall is broken down and metabolically active trophozoite emerge[1, 7]. Infected humans can either be asymptomatic or symptomatic, with a variety of symptoms including: acute or chronic diarrhoea, dehydration, nausea, vomiting and abdominal pain [7]. These symptoms whilst not only unpleasant, can have a lasting impact on children as chronic giardiasis can lead to malnutrition and weight loss, leading to a decline in development [8]. Globally, infection rates of *G. duodenalis* have been recorded between approximately 2-5% in developed countries. Consequently, developing countries have recorded infection rates between 20-30%. Whilst the Australian general population has an infection rate reflective of other developed countries of 2-5%, there are significant levels of infection in some indigenous Australian communities with infection rates matching that of developing countries [9, 10]. Due to the burden of *G. duodenalis* infection on the community, *G. duodenalis* was places on the World Health Organisations (WHO) Neglected Diseases Initiative in 2006 [11].

1.2 Nomenclature and Taxonomy of *Giardia* sp.

Although *Giardia* sp. is defined as a eukaryote, it possesses prokaryote-like features. This includes the lack of compartmentalisation of metabolic processes, a mitochondria, peroxisomes and interestingly, a Golgi body [1, 12]. There are currently six identified species of *Giardia* to date, based on the morphological characteristics of the

trophozoite and/or cyst, however, only *G. duodenalis* is able to infect humans [13]. The species *G. duodenalis* can be further classified into morphologically identical, yet genetically distinct lineages termed assemblages. To date, eight have been identified (A-H), each with a defined host range outlined in (Table 1.1) [14, 15].

Assemblages A and B are the only assemblages capable of infecting humans and therefore were the focus of this project [11, 14]. Of these eight assemblages, the degree of difference between each is more significant than between some other species of *Giardia spp*. and therefore it is debated that each assemblage should be defined as separate species [6, 13]. Therefore, any further work performed on *G. duodenalis* will support this speciation debate.

Table 1.1 Currently recognised assemblages of *Giardia duodenalis*. Adapted from [13]

Assemblage	Host specificity	Proposed species name
A	Humans and other primates, livestock, cats, dogs, some wild mammals	*Giardia duodenalis*
B	Human and other primates, cats, dogs, some wild mammals	*Giardia enterica*
C	Dogs and other canids	*Giardia canis*
D	Dogs and other canids	
E	Hoofed livestock	*Giardia bovis*
F	Cats	*Giardia cati*
G	Rats	*Giardia simondi*
H	Marine mammals (pinnipeds)	Undefined

1.3 Lifecycle of *Giardia duodenalis*

Giardia duodenalis has a two-step lifecycle consisting of two developmental forms, the metabolically active trophozoite and the dormant cyst. The cyst is released into the environment in faeces, ready to be up taken by a host [11, 16]. Once ingested, the cyst becomes exposed to gastric juices and begins to undergo a process known as excystation by where a tetranucleated excyzoite begins to form, later developing into

four diploid trophozoites. The trophozoite is the form of the parasite responsible for causing disease though colonisation of the upper portion of the small intestine where they adhere to the surface of the intestine [11]. As the disease-causing trophozoite moves through the host intestine, factors including high bile, low cholesterol and increased pH cause the trophozoite to undergo a process termed encystation. This process results in a fully formed cyst that is then excreted in the host faeces, releasing the cyst into the environment, and hereby initiating the beginning of the lifecycle once again (Figure. 1.1) [5, 17, 18].

1.3.1 The Cyst

The cyst is the environmentally resistant capsule encasing the parasite and is responsible for the spread of infection [4, 17] (Figure 1.2). The cyst is an oval shaped cell measuring 7-10 µm long and 8-12 µm wide. The cyst wall itself, encapsulating the parasite is 0.3-0.5 µm thick and is internally lined with a double inner membrane as well as an outer-most membrane, the first defence to the environment termed the filamentous later [1, 3]. This filamentous layer is mainly comprised of 60% carbohydrate, β(1-3)-N-acetyl-D-galactosamine and 40% protein [6, 17, 19]. This protein portion of the cyst wall is comprised of three cyst wall proteins, termed cyst wall protein 1-3 (CWP 1-3) [20]. These CWPs are closely related in that they contain cystine-rich repeats at the C-terminus and leucine-rich repeats at the N-terminus. Additionally, the high cystine non-variant cyst protein (HCNCp) has been seen to associate with the CWPs in the cyst wall [17]. This protein differs from CWPs as it has been detected in trophozoites whereas CWPs are not [21]. Together these layers form the highly insoluble, environmentally resistant cyst wall. The cyst can survive and remain viable within the environment for weeks to months while still remaining infectious [22]. The parasite within the cyst remains dormant whilst in the environment with a metabolic rate of 10-20% of the trophozoite until up taken by a host [1, 3].

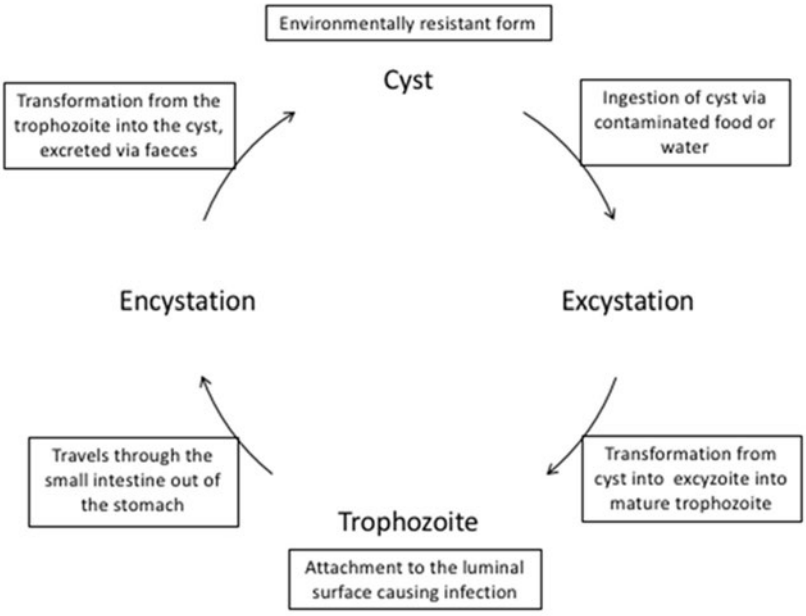

Figure 1.1. A simple representation of the lifecycle of *G. duodenalis.* The environmentally resistant cyst is ingested by a host where it starts to transition briefly into an excyzoite then finally into a metabolically active trophozoite. One it has reached the trophozoite form, *G. duodenalis* is at the disease-causing phase and begins to replicate. As *G. duodenalis* passes through the intestine, the trophozoite undergoes the second process, encystation where the trophozoite is encapsulated within an environmentally resistant cyst, before it is released into the environment, ready for uptake into a new host [17].

1.3.2 Excystation

Once ingested, the cyst undergoes a process termed excystation which produces a metabolically active form of the parasite [17]. Excystation is triggered once the cyst is ingested and exposed to the host's stomach acid [23]. As the excysting cyst reaches the small intestine, the flagella of the emerging trophozoite begin to appear through an opening in the cyst wall, followed by the body of the excyzoite, the first stage of the parasite post-excystation [4, 24, 25]. While host proteases degrade the cyst wall from the outside-in, cysteine proteases from *G. duodenalis* are thought to have in important role in the degradation of the inside of the cyst wall from the inside-out [17]. From here the newly liberated excyzoite undergoes cytokinesis where it forms four trophozoites [17]. Simultaneously as the trophozoite upregulates both its metabolism and gene expression to allow for the upregulation of proteins associated with motility to allow for structures such as the adhesive disc and flagella to function [17]. Little is known about the molecular mechanisms that regulate this rapid differentiation from a cyst to a trophozoite, though it is known to take approximately 15 minutes once initiated [17].

It is important to note that the timing of excystation is critical for the survival of the parasite as the releasing of the excyzoite within the stomach will cause the cell to lyse dur to the high pH of the stomach acid [4, 17, 24].

1.3.3 The Trophozoite

The trophozoite is the disease-causing stage of *G. duodenalis*, formed through excystation of the cyst. The trophozoite resembles a lengthwise bisected pear, with the convex side termed the dorsal surface and the flat side termed the ventral surface [6, 17]. The size of the trophozoite (Figure 1.2) is approximately 5-9µm wide, 12-15µm long and contains a median body which is characterised by its smile-like feature gives to the parasite though currently there is no known function of the median body [17]. Four pairs of flagella (anterior, caudal, posterior and ventral) emerging from the basal body allowing for motility outlined [3]. The trophozoite of *G. duodenalis* attaches to the intestinal mucosal layer via the ventral adhesive disc [1, 3]. The adhesive disc is a rigid structure whereas the outer rim surrounding the disc is flexible in its attachment to the

host intestine. Both the flagella and adhesive disc are composed of proteins similar to α-tubulin and β-tubulin two common cytockeleton proteins from the giardian family unique to the *Giardia* spp. (α-giardian, β-giardian, γ-giardian and δ-giardian) [17]. Trophozoites are seen to contain two nuclei, lacking nucleoli, located symmetrically on either-side of the midline [1, 3]. The structural elements of the trophozoite are critical to ensure the parasite can remain within the upper small intestine and avoid peristaltic elimination though the use of flagella and the adhesive disc [17].

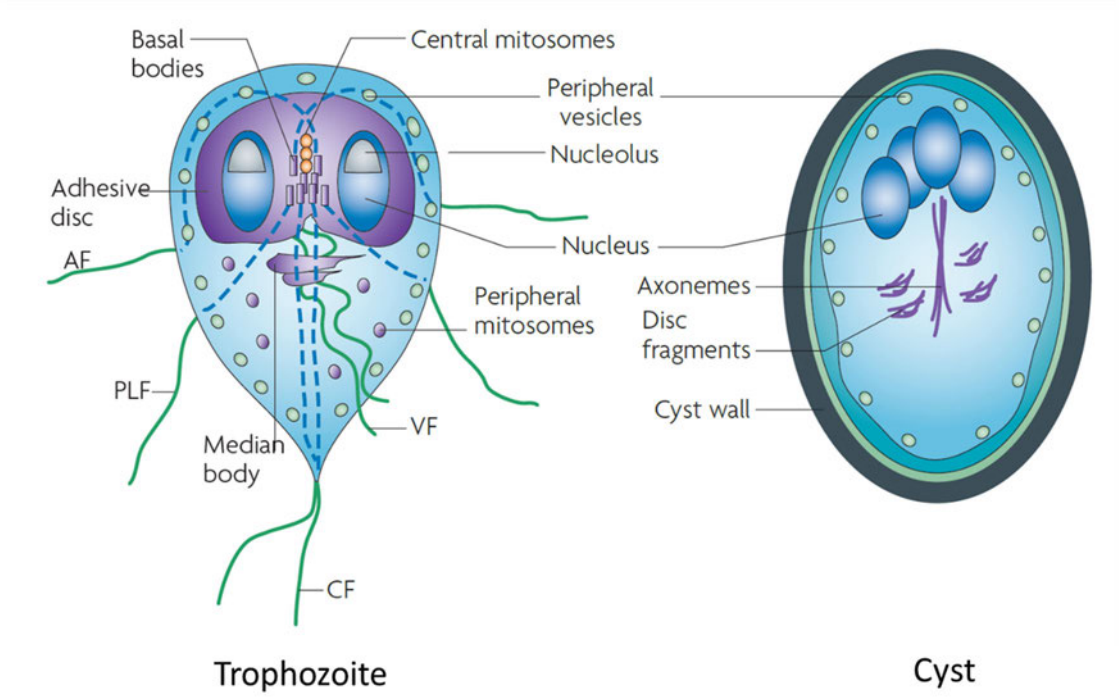

Figure 1.2. Comparative image of the two morphological and metabolically stages of *G. duodenalis*, the trophozoite and the cyst, Adapted from[17]

1.3.4 Encystation

Encystation is a critical process within the lifecycle of *G. duodenalis* as it is the developmental process where a metabolically active trophozoite differentiates into an environmentally resistant cyst which is then excreted into the environment with the goal of infecting a new host [5, 16, 21, 24]. This stage of the *G. duodenalis* lifecycle is critical for the survival of the parasite as the trophozoite is not environmentally resistant and would therefore lyse when exposed to the environment. Consequently, encystation can be thought of as a stress response in the life cycle of *G. duodenalis*. To date, encystation is thought to be triggered by a combination of host-specific factors such as high levels of bile, increased pH and low levels of cholesterol [17].

Unlike excystation which is a rapid process, encystation is a longer biological differentiation [17]. Encystation is the synthesis, packaging and export of cyst wall components to the cell wall to allow for the formation of the cyst wall [26]. This process can be broken down into three phases. Firstly, once initiated, genes specific to encystation are upregulated to allow the synthesis of various cyst wall components such as the cyst wall proteins (CWP 1-3) and the carbohydrate N-acetylgalactosamine [27]. Following this, the secretory organelles responsible for the trafficking of these newly synthesised components are produced. The main secretory organelle being the encystation specific vesicles (ESVs) [4, 5, 21, 24, 27]. ESVs are considered a rudimentary Golgi in *G. duodenalis* and are approximately 1µm in diameter and are not present in the trophozoite. It is believed that the ESVs are formed from the ER as condensed cisternae during encystation before maturing, packaging and trafficking the cyst wall components, the CWPs, carbohydrates and the HCNCp where they are destined for the cell wall [28]. Finally, these cyst wall components are targeted towards the cell periphery where they are assembled to form the environmentally resistant cyst wall [4, 27, 28]. Currently, the intracellular signal responsible for initiating this trafficking process is not yet known.

During the latter phase of encystation the morphological structures such as the cytoskeleton, adhesive disc and flagella are disassembled and internalised as the trophozoite begins to round up [16]. Once this process begins and these structures begin to be disassembled the parasite is no longer able to attach to the host intestine. From

here it is critical that the process of encystation is regulated and performed to an end point of the environmentally resistant cyst destined for excretion, as the cyst is not metabolically active and not capable of receiving nutrients from the host. Furthermore, the nuclei are divided and undergo DNA replication giving rise to a mature cyst consisting of four tetraploid nuclei [4]. In the final stages of encystation, the cyst wall proteins and the cyst wall sugars form strong interactions generating a highly insoluble 'hardy' environmentally resistant cyst wall [4].

The interesting feature of encystation is that it is the only known regulated trafficking pathway present in *G. duodenalis* and only occurs in encysting cells. Though the underlying molecular mechanisms that regulate this process are not understood.

1.4 The Golgi apparatus and the secretory pathway in eukaryotes

Given that *Giardia* spp. sit as one of the earliest divergent eukaryotes, it is hypothesised that they may possess a secretory pathway similar to that of higher eukaryotes. In support of this notion, is the utilisation of ESVs during encystation, where classical membrane trafficking seems to occur via a direct path from the endoplasmic reticulum (ER) to the Golgi and then to the plasma membrane [21]. Investigation into the molecular mechanisms of encystation and specifically the role of ESVs in a Golgi-like role may elucidate a prototypic secretory pathway within *Giardia duodenalis*.

The Golgi complex is important for eukaryotic cellular functions as it serves as a central trafficking hub of the cell. The Golgi structurally consists of polarised, flattened disc shaped membranes termed cisternae and it exists across eukaryotes. This complex can exist in three diverse morphologies, a singular unit, found in some fungi, such as *S. cerevisiae.* A laterally-linked ribbon shape comprised of a stack of multiple cisternae found in mammalian cells and thirdly in stacks of unlinked cisternae, such as in plants and insects [29].

Though the structure of the Golgi can vary between organisms, the function remains highly conserved; that is that it serves as the site at which secretory cargo is processed and organised prior to delivery to its target site. [29, 30].

1.4.1 Phosphoinositides and the secretory pathway

Eukaryotic cells rely on a distinct lipid composition within their membrane bound organelles to perform numerous intracellular activities such as protein sorting into appropriate organelles and trafficking between membranes [29, 31]. Of these lipids that make up this distinct composition, sterols, sphingolipids, and phospholipids make up the majority of the lipid environment. More specifically, phospholipids in the form of phosphoinositides (PIPs) are present in all eukaryotes with phosphatidylinositol (PtdIns) making up approximately 8% of total cellular phospholipid [29, 32]. Mammalian cells synthesise seven phosphorylated derivatives of PtdIns (PtdIns-3-P, PtdIns-4-P, PtdIns-5-P, PtdIns-3,5-P, PtdIns-4,5-P, PtdIns-3,4P_2 and PtdIns-3,4,5-P_3), whereas *S. cerevisiae* synthesise each of these with the exception of PtdIns3,4P_2 and PtdIns3,4,5P_3. Phosphoinositides are synthesised though a series of reversible reactions through the use of phosphatases and kinases that process specific headgroups [32].

One process that is of particular interest to this study is the regulation of membrane trafficking via the major PIP, PtdIns-4-P. The major site of PtdIns-4-P synthesis is the *trans*-Golgi Network (TGN) where it is produced by the PtdIns-4-OH kinase (PtdIns-4-OH kinase IIα and PtdIns-4-OH kinase IIIβ in mammalian cells with the equivalent in yeast being Pik1p) [29]. PtdIns-4-P was firstly characterised as a precursor for PtdIns-4,5-P, however its importance is now understood as an integral part of the secretory pathway. For examples, PtdIns-4-P has been shown to be an important factor for the recruitment of proteins required for secretory function as well as trafficking from the Golgi, targeting to the plasma membrane [29, 33]. These proteins include pleckstrin-homology (PH) domain-containing proteins such as the oxysterol-binding protein (OSBP) and the ceramide transfer protein (CERT) that bind to specific inositol groups aiding in membrane deformation and lipid transport [29, 32].

The process behind how these PIPs signal a wide variety of cellular functions is not completely understood though the importance of these PIPs was first demonstrated in *S. cerevisiae* where the use of phosphatidylinositol transfer proteins (PITPs), Sec14 was exhibited [30, 34, 35]. Furthermore, PIPs were determined to be crucial for cellular function and in particular, this was demonstrated in *S. cerevisiae* where the disruption

of the PtdIns-4-OH kinase (Pik1p) resulted in inhibited cell growth [29]. In addition, similar studies investigating temperature sensitive mutations of Sec14p, associated with reduced synthesis of PtdIns-4-P saw a rescue of this restrictive growth through over expressing the PtdIns-4-OH kinase, Pik1p or alternatively through the deletion of the PtdIns-4-P phosphatase Sac1p [29]. Given these discoveries, it has recently been accepted that PITPs are a major component in the biological outcomes of PIPs [35-37].

1.4.2 Phosphatidylinositol Transfer Proteins and the secretory pathway

Upon the discovery of PITPs, studies have been dedicated to the understanding of the functional roles of PITPs. PITPs were originally characterised as classical family of lipid transport proteins, responsible for the energy-independent transfer of lipids from one membrane to another. Specifically, the transfer of PtdIns and phosphatidylcholine (PtdCho) between two lipid bilayers [29, 38, 39]. This transfer of PtdIns and PtdCho from one membrane to another allows the alteration of the lipid concentration within these membranes without the input of energy [40]. PITPs were characterised as proteins that perform this activity through the use of a "transfer-assay" [1, 30, 36, 37, 41].

This original proposed function can be explained through the "lipid exchange" or "counter-flow" model that describes process of energy-independent transfer of PtdIns and PtdCho between two membranes, therefore transferring lipids from an area of high concentration to that of a low concentration *in vitro* to facilitate a specific lipid environment in membranes [35, 42]. Additionally, PITPs were seen as a crucial component in the solubilisation of lipids to allow their transfer through an aqueous environment. This has been seen to occur from the Endoplasmic Reticulum (ER) to promote Golgi function and maintain lipid homeostasis (Figure 1.3) [38, 43].

Applying the *in vitro* activity of PITPs to an intracellular function: the soluble form of PITP bound to PtdCho senses the elevated concentration of PtdIns in the donor membrane, the ER. Here the protein docks onto the ER membrane and exchanges the molecule of PtdCho with PtdIns. PITP bound to PtdIns dissociates from the ER membrane with the lipid loaded into its hydrophobic cavity. Here the PITP is in its 'closed' conformation [41]. As the protein docks onto the target membrane, it undergoes a conformational change from a closed to an open structure. At this point the bound

molecule of PtdIns is exposed to the lipid environment of the target membrane where it is subsequently discharged into its outer leaflet. After this, with the target membrane at a higher concentration of PtdCho than PtdIns, the PITP is reloaded with PtdCho into its lipid binding pocket [44]. Again, this triggers a conformational change in the protein from an open to a closed state resulting in the dissociation of PITP from the target membrane. From here the cycle can be repeated [41]. It is important to state that the energy independence of this process stems from the hydrophobic property of the interior of the PITP. The hydrophobicity of the lipid binding cleft mimics that of a membrane. Therefore, these lipids are able to process via a trajectory tailored to the environmental needs of these amphipathic molecules during the lipid exchange process [31].

This original model was later reviewed and PITPs were characterised not exclusively as passive lipid transfer proteins responsible for trafficking PtdIns between membranes, but instead as molecules that chaperone the tightly regulated synthesis of PIPs [44, 45]. The biological functions regulated by this activity include membrane trafficking, lipid droplet metabolism and membrane biogenesis [32]. The characterisation of the major *S. cerevisiae* PITP Sec14p elucidated this new proposed function of PITPs. Here the heterotypic exchange of PtdIns with PtdCho was proposed to result in the presentation of the PtdIns to PtdIns 4-OH kinase (Figure 1.4). Sec14p was shown to bind the headgroup of PtdIns and PtdCho at specific sites within the lipid binding pocket. Initially, Sec14 binds to PtdCho which prepared the protein for heterotypic exchange with PtdIns [46]. During this heterotypic exchange, the PtdIns begins to leave the lipid bilayer where it is presented to the membrane associated PtdIns-4-P OH kinase in a more accessible confirmation than when it is buried within the lipid bilayer, to allow for PtdIns-4-P production [29, 47].

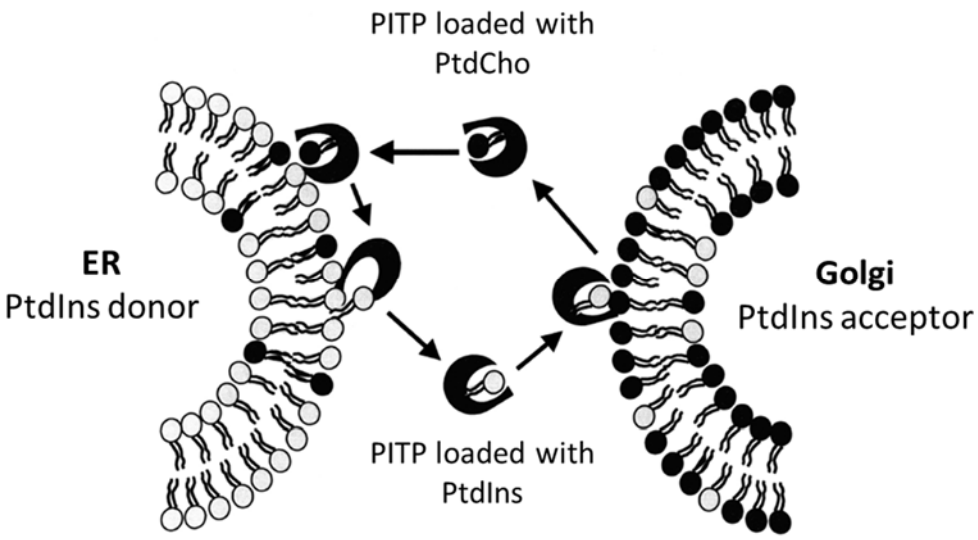

Figure 1.3. Lipid-exchange of PtdIns and PtdCho between two membranes (ER and Golgi) from an area from high concentration of PtdIns to an area of low PtdIns to promote Golgi function. Adapted from [44]

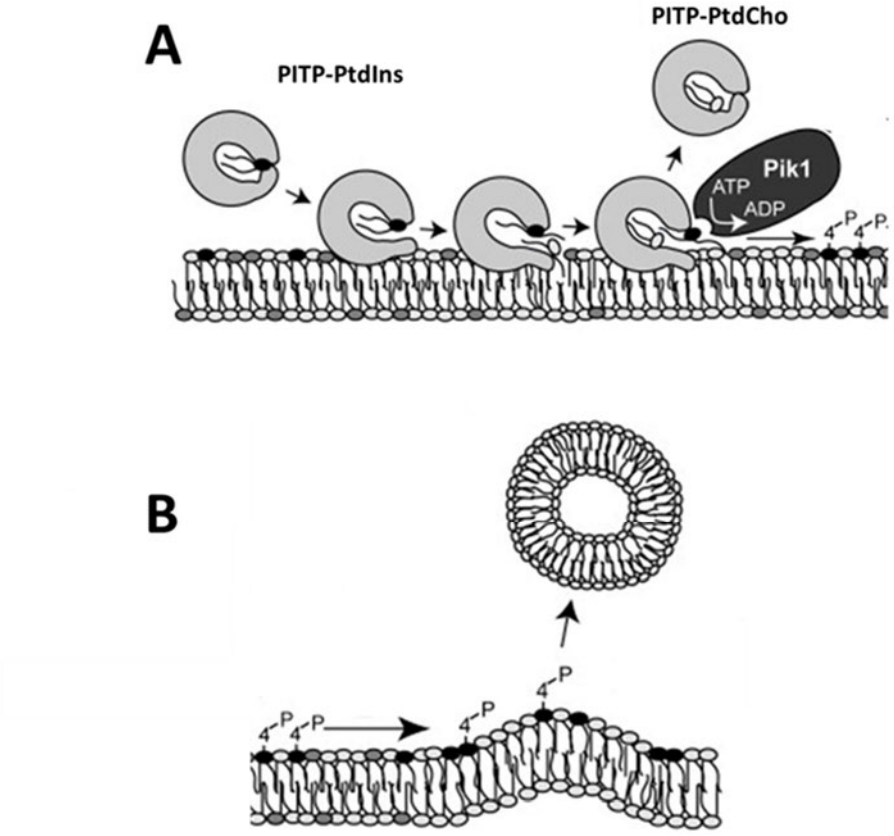

Figure 1.4. Figure outlining vesicle formation through the activity of a PITP, adapted from Grabon *et al* [45]. **A.** The PITP, pre-loaded with PtdIns approaches the membrane where it undergoes heterotypical exchange where the PtdIns within the binding pocket swabs with a PtdCho from the membrane. As the PtdIns leaves the binding pocket, it is introduced to Pik1, where it is phosphorylated into PtdIns-4-P. **B.** As more PtdIns-4-P is produced, co-proteins are recruited to aid in the destabilisation of the membrane, leading to vesicle formation [45].

Whether PITPs are strictly characterised as lipid transfer proteins or work as presentation molecules to present PIPs to required enzymes to perform functions, it is clear that PITPs play an important role in coordinating PIP metabolism with physiological outcomes [45]. Additionally, PITPs can be understood as important molecules in all cellular activities that maintain lipid homeostasis of the secretory compartments to ensure appropriate function.

1.5 Phosphatidylinositol Transfer Proteins (PITPs)

PITPs are the key lipid signalling regulators in eukaryotic cells that are approximately 35 kDa in size [48]. PITPs bind to PtdIns as well as a counter ligand. This counter ligand may either be a lipid, such as phosphatidylcholine (PtdCho) or a lipophilic molecule such as αTocopherol/Vitamin E [30, 36, 43, 49]. PITPs are found in all Eukaryotes and can be broken into two major groups based on their binding activity: the classical PITPs, characterised by their ability to bind to PtdIns and PtdCho and the non-classical PITPs that also bind to PtdIns but not PtdCho, and therefore a different counter ligand [29, 36, 47, 50, 51]. This classification of this protein super family can be further broken down into two structural branches: the Sec14-like PITPs and the genetically unrelated StART-like (StAR-related lipid transfer domain) PITPs (Figure 1.5) [29, 47].

1.5.1 The Sec14 like PITPs

The Sec14-like PITPs are a group of PITPs founded from the highly characterised yeast PITP, Sec14p, making up the Sec14 superfamily. Most of our understanding of PITPs comes from studies of Sec14 and its superfamily [29]. Sec14's fundamental function is through its localisation to the TGN where it is responsible for regulating vesicle budding and biogenesis [29, 42, 45]. This is performed through the heterotypic exchange of PtdIns and PtdCho. During heterotypic exchange, the headgroup of PtdIns as the phospholipid is either exiting or entering the binding pocket adopts a transitional state that makes it more accessible to the active site of the PtdIns-4-OH kinase. This activity results in a localised pool of PtdIns-4-P. Furthermore, this localised pool of

PtdIns-4-P promotes the maturation of secretory vesicles [29]. In addition to Sec14p, the yeast genome encodes for 5 genes encoding Sec Fourteen Homologues (SFH 1-5) [52]. Each of these SFH proteins possess PITP activity but differ in their binding activity as they do not transfer PtdCho. Furthermore, it is suggested that some of these SFH proteins may play a similar role to Sec14 in the Golgi where as others may have a more unique role, such as Sfh3 that localises to lipid droplets [48, 53]. This revealed that multiple PITPs within *S. cerevisiae* serve a diverse role in PtdIns-4-P signalling. To date there have been at least 1500 Sec14-like PITPs identified throughout eukaryotes and it must be understood that not all Sec14-like PITPs are classical in their activity. Some Sec14-like PITPs have been shown to bind to various other hydrophobic ligands such as squalene and α-tocopherol. The importance of these PITPs can be demonstrated through the loss of proper Sec14 function can lead to disrupted secretory function leading to altered cell growth or cell death[29].

1.5.2 The Metazoan StART-like PITPs

The second classification of PITPs characterised based on structure was the Metazoan PITPs, named as they were first discovered in metazoan organisms (multicellular organisms). As research into these PITPs progressed, this name was reviewed and changed to the StART-like PITPs as they were discovered in a large range of organisms [54]. The StART-like PITPs were first classified upon the identification of the first mammalian StART-like PITP. To date, numerous StART-like PITPs have been identified in eukaryotes, though not in yeast [29]. These StART-like PITPs can be further subdivided into the type I and type II. Type I StART-like PITPs are small (approximately 35 kDa) soluble proteins. These proteins are closely related to PITPα and PITPβ and bind to PtdIns and PtdCho. On the other hand, the type II StART-like PITPs are larger multi-domain membrane bound insoluble proteins that bind PtdIns and PtdOH though still have a low affinity to bind PtdCho and are therefore considered classical PITPs. The type I and type II StART-like PITP have a homologous region in their N-termini [29].

Though these two families of proteins are structurally unrelated, they both have the ability to bind and transfer PtdIns between membranes [32]. To date, all StART-like

PITPs have been classed as classical, though PITPs classed as Sec14-like PITPs have included both the classical and non-classical PITPs [47].

The mammalian PITPα and PITPβ are to date the best studied StART-like PITPs both being classical PITPs however both have the ability to bind alternative counter ligand sphingomyelin [29]. Furthermore, studies have shown that various PITP isoforms have specific localisation within the cell to perform specific functions. For example PITPα localises to the cytoplasm whereas PITPβ localises to the Golgi, TGN and the cytoplasm [29]. Interestingly it has been observed that some PITPs have overlapping function and can be substituted for one another. For example, the yeast Sec14p PITP can be substituted for the mammalian PITPα in temperature sensitive mutants with rescued growth seen [29].

As described above, PITP are a large class of proteins responsible for chaperoning a variety of tightly regulated biological outcomes involving PIPs. Given the importance of PITPs in secretory function of Eukaryotes, it would be fair to assume to apply the importance of PITPs even in the earliest Eukaryotes that are seemingly devoid of a classical Eukaryote secretory pathway.

1.6 PITPs and *Giardia duodenalis*

As previously mentioned, *G. duodenalis* undergoes a stress response known as encystation, the developmental pathway that leads to the spread of infection. Though this process is known to allow for the spread of infection and the implication of prolonged infection can lead to serious outcomes, the molecular mechanisms behind encystation are poorly understood. A study by Faso *et al.,* 2013 investigated this through a whole cell proteomic screen and found, in particular, that the *Giardia* spp. PITP (*Gd* PITP) was upregulated during encystation. The function of PITPs in *G. duodenalis* is currently unknown, therefore we must consider the role of PITPs in other eukaryotic organisms to postulate a role for these proteins in this organism. As previously mentioned, the essential *SEC14* gene in *S. cerevisiae* encodes for a 'classical' PITP [55]. Sec14 is the founding member of the Sec14-like PITPs and is highly characterised and therefore is used as a model to determine the function of other PITPs. Sec14 activity is essential to increase PtdIns-4-P synthesis in the

TGN/endosomes which is a necessary process to promote vesicle transport from these organelles and towards the plasma membrane [36, 37].

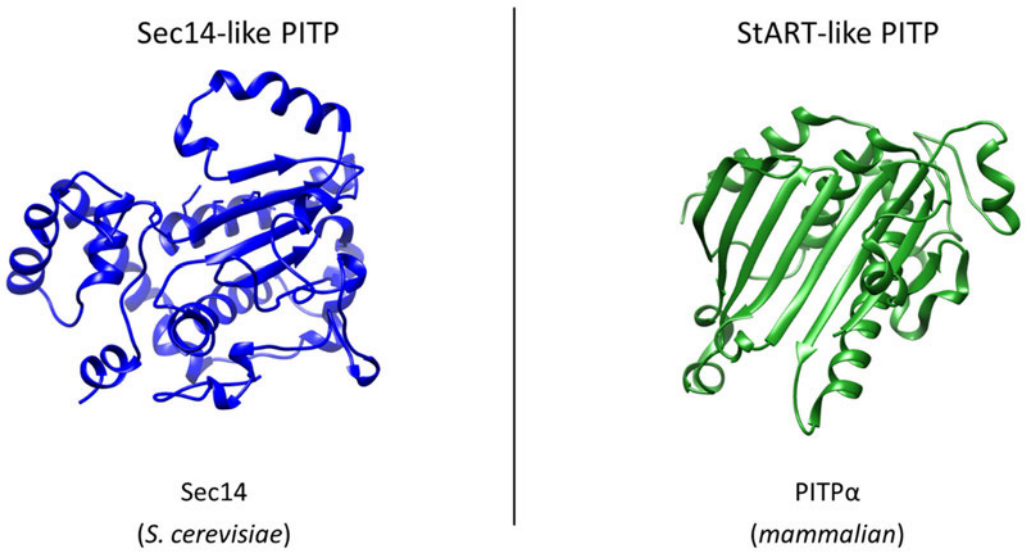

Figure 1.5. Comparison of tertiary structure of two classical PITPs, Sec14-like PITP, Sec14p and a StART-like PITP, PITPα.

1.7 Aims of this study

As mentioned, little is known about the molecular mechanisms that regulate encystation in *G. duodenalis*. However, whole cell proteomic analysis by Faso *et al*., 2013 reported the increased expression of *Gd* PITP in encysting cells specifically that may provide a hint into its role in *G. duodenalis*. Understanding how *Gd* PITP is involved in the mechanisms of encystation may aid in identifying novel regulators of this process. We hypothesised that *Gd* PITP dependant PtdIns-4-P production may be essential to promote trafficking of CWPs to the cell periphery during encystation.

To determine the role of *Gd* PITP during encystation, we initially aimed to characterise the lipid binding properties of the putative *Giardia* PITP. This was investigated through the utilisation of the model organism *S. cerevisiae* perform biochemical assays such as heterologous expression of *Gd* PITP in various temperature sensitive yeast mutants. From here a non-target and targeted approach was adopted to further characterise the lipid binding activity of *Gd* PITP.

Furthermore, we aimed to determine whether *Gd* PITP is required during encystation. To approach this objective the gene expression of *Gd* PTIP was investigated in cells undergoing encystation. Furthermore, a puromycin selectable expression vector was under construction to allow for the visualisation of the co-localisation of fluorescently labelled *Gd* PITP as well as PtdIns-4-P.

Overall, the main aim of this study was to identify key regulators during encystation, such as *Gd* PITP. Achieving this may not only elucidate the evolution of this protein and aid as a model for PITPs in higher Eukaryotes but identifying a potential target for pharmaceutical intervention may aid in diminishing the ability of *G. duodenalis* to complete encystation, therefore ablating environmental resistance.

Chapter 2

Materials and methods

2.1 Media

2.1.1 *Escherichia coli* Media

E. coli strains containing a plasmid were cultured in Lysogeny Broth (LB) 2 % agar or liquid, both containing Ampicillin 200 µg/mL and incubated at 37 °C.

2.1.2 *S. cerevisiae* Media

Yeast strains were cultured in Yeast Peptone (YP) containing 2 % glucose (YPD) overnight at 30 °C with light shaking**.** Yeast strains containing a yeast expression vector were grown at 30 °C in Yeast Nitrogen Base (YNB) containing 20 % glucose and supplemented with amino acids as required for growth excluding uracil (Ura) as per selection (YNB^{-Ura}; 0.17 % w/v yeast nitrogen base, 0.5 % w/v ammonium sulphate, 2 % w/v D-glucose, 0.002 % w/v Ade, His, Leu, Lys, Trp). Yeast strains cultured on agar were grown as above on plates containing either YPD + 2 % agar or YNB^{-Ura} + 2 % agar.

2.1.3 *G. duodenalis* Media

Giardia duodenalis trophozoites were cultured in BS-I-33 *Giardia* growth media (30 g/L biosate peptone, 10 g/L glucose, 2 g/L NaCl, 2 g/L cysteine HCl, 1 g/L K_2HPO_4, 0.6 g/L KH_2PO_4, 0.01 g/L ferric ammonium citrate, 0.2 g/L ascorbic acid, 0.5 g/L bovine bile). All cultures were grown in 15 mL borosilicate glass screw cap tubes. Cultures were incubated at 37 °C on a 45 ° incline.

2.2 Bacterial plasmids and isolates, Yeast strains and *G. duodenalis* isolates

2.2.1 *E.coli* strains and plasmids

The E.coli strains and plasmids used in this study are listed in Table 1.1

Table 2.1 E.coli strains and plasmids

Strain/plasmid	**Description**
XL-10 Gold	Ultracompetent *E.coli* cells
BL21-DE3	Competent *E.coli* T7 expression strain
pET16B	Bacterial vector utilised for inducible expression of N-terminally 10xHis tagged protein
pDR195	Yeast expression vector utilising the *PMA1* promotor

pDR195_*Gd* PITP A	Yeast expression vector placing *Gd* PITP A gene under the *PMA1* promotor
pDR195_*Gd* PITP A^{T64D}	Yeast expression vector placing *Gd* PITP A^{T64D} gene under the *PMA1* promotor
pDR195_*Gd* PITP B	Yeast expression vector placing *Gd* PITP B gene under the *PMA1* promotor
pDR195_*Gd* PITP B^{T64D}	Yeast expression vector placing *Gd* PITP B^{T64D} gene under the *PMA1* promotor
pET16B_*Gd* PITPA	Bacterial vector utilised for inducible expression of N-terminally 10xHis *Gd* PITP A protein
pET16B _*Gd* $PITPA^{T64D}$	Bacterial vector utilised for inducible expression of N-terminally 10xHis *Gd* PITP A^{T64D}
pET16B _*Gd* PITPB	Bacterial vector utilised for inducible expression of N-terminally 10xHis *Gd* PITP B
pET16B _*Gd* $PITPB^{T64D}$	Bacterial vector utilised for inducible expression of N-terminally 10xHis *Gd* PITP B^{T64D}

2.2.2 Yeast strains

S. cerevisiae strains used in this study are listed in Table 2.2

Table 2.2 *S. cerevisiae* strains

Yeast strain	**Description**
BY4742	Wild-type control
Sec14-1ts	*ts* mutant of the *SEC14*. A gene encoding for the yeast PITP Sec14p
Pik1-101ts	*ts* mutant of the *PIK1*. A gene encoding for the yeast PtdIns-4-P kinase Pik1p
sfh3Δ	Knock our strain of *SFH3* derived from CTY182 strain

2.2.3 *G. duodenalis* isolates

Giardia duodenalis strains used in this study listed in Table 2.3

Table 2.3 *G. duodenalis* strains

***G. duodenalis* isolate**	**Description**
BAH 2c2	Assemblage A
BAH 34c8	Assemblage B

2.3 Storage and maintenance of bacterial isolates, yeast strains and *G. duodenalis* isolates

2.3.1 Storage of strains

Strains and plasmids were grown to stationary phase in LB at 37 °C (*E. coli*) or in YPD at 30 °C (*S. cerevisiae*). 500 µL aliquots of the culture were mixed with 500 µL of 50 % glycerol in Nalgene cryogenic vials and stored at -80°C.

2.3.2 Maintenance of *G. duodenalis* cultures

Giardia duodenalis isolates were obtained from Murdoch University and listed in Table 2.3. *Giardia duodenalis* isolates were grown at 37 °C on a 45 ° incline and sub cultured every 3-4 days or as cultures become confluent.

Confluent cultures were left on ice for 30 minutes to detach trophozoites from the side of the glass culture tubes. The tubes were then inverted to mix trophozoites throughout media and 0.5 – 1.0 mL of this mix was used to inoculate 14 mL of pre-warmed 0.22 µm filter sterilised media contained within a 15 mL borosilicate glass screw cap tube

2.3.3 Cryopreservation of *G. duodenalis* trophozoites

A confluent 15 mL culture of *G. duodenalis* was incubated on ice for 30 minutes. After incubation, the culture tube was inverted several times and moved into a 15 mL falcon tube and centrifuged for 10 minutes at 1 000 x g at 4°C.

Supernatant removed and 6 mL of 7.5 % DMSO in 37 °C 0.2 µM filter sterilised growth media. 1 mL aliquots of the cell suspension was added to cryopreservation tubes and left at -80 °C overnight. Following this, tubes were moved to liquid nitrogen for long term storage.

2.3.4 Culturing of *G. duodenalis* trophozoites post-cryopreservation

Cryopreservation tubes were removed from liquid nitrogen and left to defrost at room temperature. 14 mL of 37 °C growth media was 0.2 µM filter sterilised into 15 mL glass culture tubes. 500 µL of the defrosted trophozoites were aliquoted into the culture tube containing growth media and mixed via inversion.

Culture tubes were incubated at a 45 ° incline at 37 °C and monitored until confluent, approximately 2-4 days.

2.4 Spectroscopy

Optical densities of *E. coli* and *S. cerevisiae* cultures were determined using BioPhotomoter plus (VWR) measuring absorbance at 600 nm. Nucleic acid concentrations were determined using a Nanodrop ND-1000.

2.5 DNA and RNA manipulation

2.5.1 Electrophoresis

All polymerase chain reaction (PCR), cut and uncut plasmid DNA and restriction enzyme-digested DNA was mixed with DNA loading dye (2 % w/v Bromophenol Blue, 30 % Glycerol) and separated on 1-2% (w/v) agarose gels made with and run in Tris-acetate (TAE) buffer (40 mM Tris, 20 mM acetate, 1 mM EDTA pH 8.6) containing 0.1 µg/mL gel green. 2 µL of 2-log DNA ladder was run alongside samples.

Following electrophoresis, DNA was visualised using UV transilluminator and image recorded using the BioRad Chemidoc Gel Documentation system.

2.5.2 *Giardia* DNA extraction

A confluent 15 mL culture of *G. duodenalis* cells is incubated on ice for 30 minutes to detach cells from the side of the tube. Cells were transferred to a 15 mL falcon and centrifuged at 12 000 x g for 10 minutes and supernatant discarded. Cells were resuspended in 200 µL of ddH_2O and transferred to a screw cap tube and approximately 100 µL of acid washed glass beads were added to the tube. The tube was placed in a MP FastPrep® set to speed 6 m/sec, Quickprep adapter for 40 seconds. The lysed cells were transferred to a 1.5 mL microcentrifuge tube without the glass beads. 200 µL of 5 M potassium acetate was added to the tube and the sample was incubated on ice for 1 hour. After incubation, the sample was centrifuged 12 000 x g for 5 minutes at 4 °C. The supernatant was then transferred to a 1.5 mL microcentrifuge tube and an equal volume of room temperature isopropanol was added to the tube, mixed, and incubated at room temperature for 5 minutes. After incubation, the sample was centrifuged at 12 000 x g for 10 seconds at 4 °C, supernatant removed, and the pellet left to air dry for approximately 10 minutes. Once dry, the pellet was dissolved in TE (pH 8.0) containing 20 µg/mL pancreatic RNase and incubated at 37 °C for 30 minutes. After incubation, 30 µL of 3 M sodium acetate (pH 7.0) was added to the sample, mixed with inversion then 200 µL of isopropanol added. The tube was immediately centrifuged at 12 000 x g for 20 seconds at 4 °C. Supernatant was

removed and the pellet air dried for approximately 10 minutes. Once dry, DNA was dissolved with 150 µL of TE (pH 7.4).

2.5.3 Commercial plasmid purification kits

Plasmid DNA was isolated from E. coli cultures using FavorPrep™ Plasmid Extraction Mini Kit (Favogen®) according to manufacturer's instructions and plasmid DNA was eluted in 50 µL ddH_2O.

2.5.4 Commercial PCR purification kit

PCR product was purified using an Isolate II PCR and Gel Kit (Bioline) according to manufacturer's instructions and PCR product was eluted in 15 µL ddH_2O.

2.5.5 Restriction endonuclease digestion

Plasmid DNA preparations were digested with restriction enzymes (New England Biolabs) and CutSmart buffer and incubated between 60-90 minutes at 37°C. Digested vector DNA was used for cloning in experiments to follow.

XhoI and BamHI restriction endonucleases were used for digesting the yeast vector pDR195 and inserting sequences encoding PITP A and PITP B and associated mutations (Figure 3.3). BamH1 and NdeI were used to digest the *E.coli* expression vector pET16b and inserting sequences for PITP A, PITP B and associated mutations (Figure 4.1).

2.5.6 Ligations

Ligations were performed to clone PCR product and/or restriction endonuclease digested product into various expression vectors. Ligation mixes were made containing (1 µL ligase, 1 µL ligase buffer, 1 µL plasmid DNA, 3 µL insert product, made up to 10 µL H_2O) with a negative containing all components with the product substituted with H_2O. Ligase reaction was incubated at 16 °C for 12-16 hours. Following incubation, ligase mix along with negative control was transformed according to bacterial chemical competent transformation protocol previously mentioned.

2.5.7 Tri-Reagent RNA isolation

A confluent 15 mL culture of *G. duodenalis* cells is incubated on ice for 30 minutes to detach cells from the side of the tube. Cells were transferred to a 15 mL falcon and

centrifuged at 12 000 x g for 10 minutes and supernatant discarded. Cell pellet was washed with 200 µL of PBS and transferred to a 1.5 mL microcentrifuge tube and centrifuged one more. 500 µL of TRIzol™ Reagent was added to the sample and mixed by inversion. The sample then underwent 5 cycles of freeze-thawing which consisted of freezing in liquid nitrogen and thawing to 58 °C on a heat block.

On last cycle, sample was left at room temperature after thawing then 100 µL of chloroform was added to the sample and mixed vigorously for 15 seconds then incubated at room temperature for 15 minutes. Sample was then centrifuged at 12 000 x g for 15 minutes at 4 °C. The sample will then be separated into three layers, the pink organic phase, the interphase containing DNA and the upper aqueous laying containing RNA. The aqueous layer was transferred to a fresh 1.5 mL microcentrifuge tube and 250 µL of isopropanol was added to the tube and mixed with inversion.

The sample was then stored overnight at -20 °C to precipitate RNA. After incubation, the sample was centrifuged at 12 000 x g for 30 minutes at 4 °C. The supernatant was removed, being careful to not disturb the pellet. The pellet was then washed with 1 mL of 70 % EtOH (v/v) and mixed by flicking the tube. The sample was then centrifuged at 7 500 x g for 5 minutes at 4°C.

The EtOH was carefully removed, and the sample was dried using a vacufuge for 30 minutes. The RNA was dissolved in 26 µL of RNase free H_2O. RNA was stored at -80 °C until required.

2.6 Polymerase Chain Reaction (PCR)

PCR was utilised for amplification of DNA for cloning, sequencing, primer optimisation for quantitative PCR (QPCR) and screening of plasmid clones.

QPCR was utilised to quantify relative gene expression of mRNA of *G. duodenalis* genes. Primers used for PCR, QPCR and DNA sequencing are listed in Table 2.4

Table 2.5 Oligonucleotides used in this thesis

Name	**Sequence 5' to 3'**	**Use**
qPCR primers		
qCwp 1 (A) F	GTCGAAATCTACGATGCC	qPCR
qCwp 1 (A) R	TGTTGCTCAAGTAAAGGG	qPCR
qFBA (A) F	GCATCCACCTTGACCACGGC	qPCR
qFBA (A) R	AAGTTCAGCCTCCACTGAC	qPCR
qNADH (A) F	GGCCTCACGCAAAGGGAACC	qPCR
qNADH (A) R	CTGGACATGCGCGGTCGTAA	qPCR
qTPI (A) F	TATCAAGAGCCACGTGGCGG	qPCR
qTPI (A) R	ACTTGTCTCGCCAGCCACG	qPCR
qPITP (A) f	AGTTTGCAGAGGCCAAGGGG	qPCR
qPITP (A) R	CGGTGCTTCCCTGTTCTCCT	qPCR
Amplification of *Gd* PITP A and *Gd* PITP B promotor and open reading frame primers		
Gd PITP (A) F	AAGCTTGCTTTTTGAAAATACGAAGTTGGG	PCR
Gd PITP (A) R	GATATCTCACTTGTCATCGGCCTTATCGG	PCR
Gd PITP (A) S35S F	TGGCAGCAAGGTTCTTCTCCTTAGCTTC	SDM
Gd PITP (A) S35S R	GGAGAAGAACCTTGCTGCCAAGGAGAAC	SDM
Gd PITP (A) prom F	AGCTTGCTTTTTGAAAATACGAAGTTGGGAAATTCAAAATTTG TGGTCTTAAAAACAA	PCR
Gd PITP (A) prom R	ATCGTATTTTTGTTGTCGAATATTGTTTTTAAGACACAAAATTT TGAATTTCCCAACTTC	PCR
NdeI GL50803_4197 ORF_F	CATATGCGCTACTATGTGTTTGCCATCC	Cloning
XhoI GL50803_4197 ORF_F	ctcgagATGCGCTACTATGTGTTTGCCATCC	Cloning
BamHI GL50803_4197 ORF_R	ggatccTCACTTGTCATCGGCCTTATCGG	Cloning
NdeI GL50581_3968 ORF_F	CATATGCGCTACTATGTGTTTGCCATCC	Cloning
XhoI GL50581_3968 ORF_F	ctcgagATGCGCTACTATGTGTTTGCCATCC	Cloning
BamHI GL50581_3968 ORF_R	ggatccTTACTTTTCATCAGCTTTGTCTGCG	Cloning
PITP A T64D_F	TCCGGCATCTATgaCTTTAAGCTGCTTCAC	SDM
PITP A T64D_R	GCTTAAAGtcATAGATGCCGGATTCCTCCT	SDM
PITP B T64D_F	TCTGGTATTTATgaCTTTAAAATACTTCAC	SDM
PITP B T64D_R	TTTTAAAGtcATAAATACCAGACTCCTCCT	SDM

2.6.1 Standard PCR protocol

For amplification of DNA from plasmid or genomic DNA for use in cloning, Q5 high fidelity polymerase was used. For screening and primer optimisation, *Taq* polymerase was used. For standard PCR, a total reaction volume of 20 µL reaction was used. For site directed mutagenesis (SDM) a total reaction volume of 25 µL was used. Reactions for standard *taq* polymerase PCR contained standard *taq* buffer, 10 nM of dNTP mixture, 200 nM each of the forward and reverse primer, 0.2 units of *taq* polymerase, approximately 1000 ng DNA template and the reaction volume was made up to 20 µL using milli-Q H_2O. Thermal cycling was performed using Applied Biosystems (Veriti 96-well Thermal Cycler) thermal cycler. PCR conditions were as follows: one cycle at 98 °C for 1 minute, 30 cycles of: 98 °C (10 s), 55-65 °C (30 s), 72 °C (30 s per 1 kb product) and a final cycle of: 98 °C (10 s), 55-65 °C (10-30 s), 72 °C (5 minutes). The reaction was held at 14 °C until sample was removed.

2.7. Chemical competent bacterial transformation method

40 µL of XL-10 Gold competent *E. coli* were incubated with 10 µL of plasmid DNA. The reaction was incubated at room temperature for 1 hour. After incubation, the reaction was heat shocked at 42 °C for 45 seconds then incubated on ice for 5 minutes. After incubation, reaction mix was lawn inoculated onto LB Amp plates or into LB Amp media and incubated overnight at 37 °C.

2.8 Yeast transformation

S. cerevisiae strains as listed in Table 2.2 were cultured in 10 mL of YPD overnight at 30 °C. Cells were harvested by centrifugation at 2000 x g for 5 minutes and washed with 5 mL of lithium acetate/TE solution (LiOAc/TE; 100 mM lithium acetate, 10 mM Tris pH 7.5, 1 mM EDTA) and incubated at 30°C for 1 – 2 hours with light shaking. Cells were harvested via centrifugation as previously described and resuspended in 200 µL of LiOAc/TE. Per transformation reaction required, 34 µL of the cell suspension along with 2 µL of plasmid DNA, 6 µL of 8 mg/mL single stranded salmon sperm DNA heated to 95 °C for 5 minutes and 200 µL of LiOAc/TE with 40 % (w/v) polyethylene glycol (PEG 4000) were added to a 1.5 mL microcentrifuge tube. A negative reaction was set up alongside without plasmid DNA. The reactions were vortexed to mix and incubated at room temperature for 1 hour. Following incubation,

cells were heat shocked at 42 °C for 15 minutes and plated out onto YNB^{-Ura} agar plates and incubated at 30 °C for 3 days.
Positive transformants were re-inoculated on YNB^{-Ura} agar in preparation for Serial-dilution spot test.

2.9 Serial-dilution spot tests of yeast

Yeast transformants were picked and re-struck onto selectable YNB^{-Ura} + 2 % (w/v) agar media and incubated at 30 degrees for 48 hours. One isolated colony of each transformant was picked and emulsified in 1 mL ddH20 and cell density measured at OD_{600nm}. Each emulsion was then standardised to 1 OD_{600nm} and serially diluted (1/10, 1/100, 1/1000, 1/10 000) and 10 µL was plated out on YNB^{-Ura} and grown at 30 °C, 34°C and 37°C for 3 days. Images of growth was recorded using the BioRad ChemiDoc system and analysed using the BioRad Image lab software.

2.9.1 Miconazole sensitivity of yeast

Sfh3Δ cells were transformed as per yeast transformation method 2.8. Yeast transformants were picked and re-struck onto selectable YNB^{-Ura} media and incubated at 30 degrees for 48 hours. Yeast transformants were then used for serial-dilution spot tests as method 2.9, on YNB^{-Ura} + 2 % (w/v) agar containing (0.01, 0.05, 0.1, 0.2, 0.5 µg/mL) miconazole.

2.10 Site directed mutagenesis (SDM)

Site directed mutagenesis was utilised to mutate a single nucleotide to produce the *Gd* PITP B^{T64D} mutant in the pET16b vector. Oligonucleotides (Table 2.4) used to perform SDM were designed to contain 25bp complementary sequence with the incorporated mutation within the complementary sequence and an over-hang of 8bp on the 5'end of each oligonucleotide.

PCR was used to amplify a vector containing the mutation with reactions containing (5 µL Q5 buffer, 0.2 mM dNTPs, Q5 polymerase, 1 µL plasmid DNA and made up to 25 µL with ddH_2O). Cycle conditions were

PCR product was restriction enzyme digested with DPN1 in a 10 µL reaction containing (3 µL PCR product, 0.2 µL DPN1, 1 µL CutSmart® buffer, 5.8 µL ddH_2O) and incubated at 37 °C for 2 hours. Digested product was transformed into XL-10 Gold

competent *E. coli* as per bacterial transformation method 2.9.1. and plated onto LB + 200 µg/mL Amp Agar plates and incubated at 37 °C overnight.

Single colonies were picked from these plates and cultured in LB + 200 µg/mL Amp and incubated at 37 °C overnight. Following incubation, plasmids were extracted according to 2.6.3

2.11 Microscopy

Yeast transformants containing *Gd* PITP and the mutants were picked and incubated at 30 °C in YNB^{-Ura} media to stationary growth phase.

Prior to microscopy cells were stained and fixed according to the below methods.

2.11.1 Staining of cells with BODIPY 493/530

Each transformant grown to stationary was measured at OD_{600nm} and 1 OD_{600nm} of cells were harvested and added to a 1.5 mL microcentrifuge tube. Cells were centrifuged at 12 000- g for 3 minutes, supernatant removed, and cells washed with 1 mL of PBS and harvested via centrifugation as previous. Cells were stained as per Qiu et al., 2016 with 2.5 µg/mL BODIPY™ 493/530 solution made in PBS and incubated at 37°C for 15 minutes [56]. An unstained control was performed alongside for use in flow cytometry. Cells were then harvested via centrifugation and washed with 1 mL PBS in preparation for fixation.

2.11.2 Fixation method

Cells used for microscopy and flow cytometry were fixed post-staining. Immediately following staining, cells were washed in 1 mL PBS then harvested via centrifugation and resuspended in 500 µL 3.7% (v/v) Formaldehyde solution made up in PBS. Cells were then stored at room temperature for 15 minutes. Once incubated, cells were centrifuged for 5 minutes at 8000 x g and resuspended in 500 µL PBS.

2.11.3 Concanavalin A coverslips for microscopy

To stabilise cells for microscopy, cells were adhered to Concanavalin A (Con A) coverslips. 70 µL of 10 mg/mL solution of ConA was dropped onto the centre of each glass coverslip. Coverslips were left to dry at 37 °C for approximately 30 minutes or until the coverslip is dry. Once dry, each coverslip was rinsed by dipping into ddH_2O and left to dry at 37 °C for 30 minutes or until dry.

Once dry, 40 µL of each sample stained and fixed cells were dropped onto the centre of each dry coverslip and incubated at 37 °C for 10 minutes. After incubation, coverslips were gently rinsed by dipping into ddH_2O to remove non-adherent cells and immediately mounted onto a glass slide.

Cells were viewed on the UltraVIEW microscope and imaged at 100x oil immersion under DIC and GFP settings.

2.11.4 Microscopy and imaging processing

Cells were visualised and imaged using the UltraVIEW Vox spinning disc microscope under the DIC and GFP (530 nm) channels to determine the size and presence of neutral lipids as indicated by punctate staining.

Images were processed using Image J software.

2.12 Flow Cytometry

Yeast cells stained with BODIPY™ 493/530 and unstained yeast cells prepared as previously described were used for flow cytometry.

A minimum of forty thousand cells were analysed by the FACS LSR Fortessa™ flow cytometer (BD Biosciences, Heidelberg, Germany) and data was analysed using the FlowJo™ FCS analysis software (Inivai Technologies, Melbourne, Australia). Median fluorescent intensity (MFI) BODIPY™ (530_30), FSC-A and SSC-A fluorescence was obtained after gating for BODIPY™ 493/530 positive singlets.

2.13 Protein induction

The pET16B expression vector was utilised to allow for recombinant expression of 10 x His tagged protein. pET16b vectors containing the *Gd* PITP A, *Gd* PITP B, *Gd* PITP A^{T64D} and *Gd* PITP B^{T64D} were transformed into BL21-DE3 competent *E. coli* cells as described previously and lawn inoculated onto LB + 200 µg/ mL Amp plates and incubated overnight at 37 °C. Following incubation, one colony from each plate was then cultured in 1 mL of LB + 200 µg/ mL ampicillin until stationary. A 20 mL culture of LB + 200 µg/ mL ampicillin was then inoculated to a starting OD_{600} of 0.05 cells per mL. This culture was then grown to 0.5 OD_{600} /mL at which point 0.5 OD_{600} of cells was harvested from each culture, cells harvested via centrifugation and resuspended in 50 µL of Laemmli Buffer (63 nM Tris pH6.8, 10 % (v/v) glycerol, 5 % (v/v) β-mercaptoethanol (BME), 2 % (w/v) SDS, 0.005 % (w/v) bromophenol blue)

and heated at 95°C for 5 minute. Following the sampling, the remaining culture was inoculated with 0.1 Mm Isopropyl β-D-1-thiogalactopyranoside (IPTG) IPTG. The cultures were incubated at 37 °C and sampled at 0, 1, 2, 3 and 4 hours post induction (h.p.i). These cultures were used to characterise the induction profile of each protein.

The above method was increased from 20 mL cultures to 400 mL and incubated for 16 – 18 hours for larger quantities of protein required for protein purification and protein related assays. Induced cells were harvested via centrifugation at 10 000 x g for 10 minutes and stored at -80°C in preparation for protein purification.

2.14 SDS-PAGE

10% polyacrylamide gels were used for all protein gels. Polyacrylamide gels were run using SDS running buffer (25 mM Tris, 192 mM Glycine, 0.1 % (w/v) SDS) at 25 mA per gel. 10 µL suspended in Laemmeli Buffer was loaded onto the gel alongside 5 µL of BioRad Kaleidoscope protein ladder.

Polyacrylamide gels were stained for total protein content using Coomassie brilliant blue staining solution (0.025 % (v/v) Coomassie Brilliant blue G 250, 40 % (v/v) CH_3OH and 7% (v/v) CH_3COOH) and left for 2 hours. Gels were then destained overnight using destaining solution (7 % (v/v) CH_3COOH, 5 % (v/v) CH_3OH) replacing destain every hour until protein bands become visible.

2.14.1 Western Blot

Gels required for western blotting were transferred onto PVDF membrane via a semi-dry transfer apparatus at 150 mA, 25 V for 1 hour and 30 minutes with transfer buffer (20 Mm Tris-Base, 150 mM Glycine, 20 % (w/v) MeOH).

Once protein was transferred onto the PVDF membrane, the membrane was blocked for 30 minutes – 1 hour in TBST (130 mM $NaCl_2$, 2.6 mM KCl, 2 mM Tris pH7.6, 0.1 % tween 20 (v/v)) containing 5 % (w/v) skim milk powder (TBSTM) at room temperature with shaking. TBSTM was removed and primary antibody was added to the membrane at a concentration of 1/2500 made in TBSTM and incubated at room temperature for 2 hours with shaking. Primary antibody was them removed and the membrane was washed five times, for 5 minutes each wash in TBST with shaking. Secondary antibody was then added to the membrane at a concentration of 1/10000 made in TBST and incubated at room temperature for 1 hour with shaking. Following

secondary antibody, the membrane was washed once again for 5 minutes three times in TBST. Following the final wash, 500 mL of SuperSignal® West Pico chemiluminescent substrate (Thermo Scientific) was applied to the blot before visualising using the BioRad ChemiDoc™ MP system.

2.15 Purification of polyhistidine tagged protein

Induced cell pellets were resuspended in 10 – 20 mL of ice-cold Equilibration buffer (50 mM Na_3PO_4, 300 mM $NaCl_2$, 10 mM $C_3H_4N_2$; pH 7.4) and incubated on ice for 10 minutes. The cell suspension was lysed using the Constant Systems Ltd Continuous Flow Cell Disruptor. The system was initially prepared for use by washing with 100 mL of ice-cold H_2O through the system at 130 MPa. The system was then washed with 50 mL of ice-cold equilibration buffer at 130 MPa. The cell suspension was then passed through the system twice at 137 MPa. Following lysis of cells, the cell lysate was centrifuged at 20 000 x g for 10 minutes and the supernatant passed through a 0.22 µM Millex®-GP syringe filter.

1 mL of HisPur™ Cobalt Resin was added to the filtered cell lysate and incubated at 4 °C with constant inversion for 30 minutes. The cell lysate and resin solution was transferred to a Gravity-flow Column. The stopper was removed from the bottom of the column and the flow-through was collected in a 50 mL falcon. The Gravity-flow column was then washed a total of five times, each with 5 mL of Wash buffer (50 mM Na_3PO_4, 300 mM $NaCl_2$, 10 mM $C_3H_4N_2$; pH 7.4) with the flow through collected at each step. Finally, purified protein was eluted in 1 mL twice with Elution buffer (50 mM Na_3PO_4, 300 mM $NaCl_2$, 150 mM $C_3H_4N_2$; pH 7.4.)

2.16 Yeast membrane extraction

BY4742 *S. cerevisiae* cells were grown in 400 mL of YPD to OD_{600} 0.5 – 2. Cells were harvested by centrifugation at 3000 x g for 3 minutes at 4°C. Cells were then washed with 10 mL of resuspension buffer (100 mM Tris SO_4 pH 9.4, 10 mM DTT) then resuspended in 1 mL per 50 OD_{600} of resuspension buffer and incubated at room temperature for 10 minutes.

Cells were then isolated via centrifugation at 3000 x g for 5 minutes at 4 °C and resuspended in 1 mL per OD_{600} spheroplast buffer (0.7 M $C_6H_{14}O_6$, 0.5 % (w/v) glucose, 50 mM Tris HCl pH 7.4) and 1.5 U of lyticase per OD_{600} and incubated at 30 °C for 30 minutes. After incubation, cells were centrifuged at 2500 x g for 5 minutes

at 4 °C and the sample was resuspended in 1 mL per 200 OD_{600} ice cold lysis buffer (0.1 M $C_6H_{14}O_6$, 50 mM KOAc, 20 mM HEPES pH 7.4, 2 mM EDTA and 1 mM DTT). Acid washed glass beads were added to the sample up to 75 % of the sample volume and then proceeded to have 5 cycles of vortexing for 30 second cycles and incubation on ice for 30 seconds. Following the vortexing, the sample was centrifuged at 1000 x g for 10 minutes at 4 °C to remove cell debris. The soluble fraction was retained and centrifuged at 10 000 x g for 20 minutes at 4 °C to isolate membranes. The pelleted membranes were washed twice in 1 mL of ice-cold membrane storage buffer (250 mM $C_6H_{14}O_6$, 20 mM HEPES pH 7.4, 50 mM KOAc, 1 mM DTT, 2mM MgOAc) and finally centrifuges at 10 000 x g for 20 minutes at 4 °C and resuspended to a final volume of 1 mL per 50 OD_{280} in ice-cold membrane storage buffer and snap frozen in liquid nitrogen and stored at -80 °C until required.

2.17 Lipid Binding Experiment

Purified protein was dialysed in dialysis buffer (NaH_2PO_4, $NaCl_2$) to remove imidazole. Protein was dialysed for 2 hours at 4 °C before changing buffer and leaving for 12-16 hours at 4 °C.

200 µL of 10 ng/µL stocks of proteins were made (Kes1p, $Kes1^{Y97F}$, Sec14p, PITP A, PITP B) in reaction buffer (50 mM NaH_2PO_4, 300 mM $NaCl_2$, 0.05 % (v/v) Triton™ X-100). Additionally, 1.5 mL of 100 ng/µL stock solution of TopFluor® cholesterol (Avanti Lipids) made in reaction buffer.

Protein and lipid reactions were made in triplicate containing 50 µL of protein and 50 µl of TopFluor® cholesterol in a 1.5 mL microcentrifuge tube. A negative control was made alongside containing 50 µL of reaction buffer instead of protein.

The reactions were left for 3 hours at 4 °C with constant inversion in the dark. After incubation, 20 µl of pre-equilibrated HisPur™ resin beads, washed twice with reaction buffer, were added to each reaction, and incubated at 4 °C for 1 hour in the dark to bind protein to the resin.

After incubation with HisPur™ resin beads, the beads were washed 4 times with wash buffer (50 mM NaH_2PO_4, 300 mM $NaCl_2$, 50 mM KCl), ensuring to not remove any beads. After washing, protein bound to the beads was eluted in 200 µL of elution buffer (50 mM NaH_2PO_4, 300 mM NaCl, 150 mM $C_3H_4N_2$).

100 µL of each reaction along with 100 µl of TopFluor® Cholesterol stock was added to a 96-well low fluorescent plate and fluorescent units measured on a Perkin Elmer™ Ensight plate reader.

2.18 Mass Spectroscopy sample preparation

Mass spec was used to identify lipids bound to *Gd* PITP derivatives. 1 µg of dialysed protein was added to 100 µL of yeast membranes in a 1.5 mL microcentrifuge time and made up to 500 µL with binding buffer ($NaCl_2$, NaH_2PO_4, Triton™ X-100). The reactions were incubated at 4 °C for 12-16 hours with constant inversion. After incubation, protein bound to lipids were isolated via centrifugation at 12 000 x g for 2 minutes at 4 °C. Supernatant was transferred to an ultracentrifuge tube, leaving behind the cell debris, and centrifuged at 100 000 x g for 1 hour at 4 °C. The supernatant, containing protein bound to lipids was transferred to a 1.5 mL microcentrifuge tube and 10 µL of pre-washed with binding buffer HisPur™ resin beads were added to the sample. The reaction containing beads was incubated at 4 °C for 3 hours with constant inversion. Following incubation, the beads were washed 4 times with reaction buffer (no imidazole) and finally eluted in 200 µL elution buffer. 100 µL of the elution was stored in a 1.5 µL microcentrifuge tube at 4 °C until required.

The remaining 100 µL of eluant was used for methanol/chloroform phase separation to remove lipids bound to the protein.

2.18.1 Phase separation of lipid bound to protein

Methanol/chloroform was used at a ratio of 1:2 (v/v) to separate protein and lipid. 160 µL of ice-cold methanol and 320 µL of ice-cold chloroform was added to the 100 µL of pre-eluted lipid bound to protein and mixed. The reaction was incubated on ice for 20 minutes with mixed by vortexed every 5 minutes.

After incubation, 150 µL of ddH_2O was added to the reaction, mixed, and incubated on ice for a further 10 minutes. Following incubation, sample was centrifuged at 2 000 x g for 5 minutes at 4 °C. The bottom organic layer was transferred to a fresh 1.5 µL microcentrifuge tube. The organic layer was once again centrifuges to remove any remaining aqueous layer and the organic phase transferred to a fresh 1.5 µL microcentrifuge tube.

Sample was placed into a vacufuge at room temperature and left for 30 minutes or until no residual liquid remains and a lipid film is present at the bottom of the tube. Lipid film was stored at -80 °C.

Chapter 3

Saccharomyces cerevisiae as a model to investigate *Gd* PITP

3.1 Introduction

Encystation is a critical process in the lifecycle of *G. duodenalis* as it produces an environmentally resistant cyst which is responsible for the transmission of disease [4, 5, 19, 21, 24, 26]. The underlying molecular mechanisms that control encystation are poorly understood. A study by Faso *et al*., 2013, investigating the potential molecular mechanisms involved in encystation, through whole cell proteomics analysis of *G. duodenalis* found the expression of a protein, Phosphatidylinositol (PtdIns) Transfer Protein (PITP) to be elevated during encystation [57]. As previously mentioned, ESVs play an important role in encystation. As *G. duodenalis* are void of a rudimentary Golgi apparatus, is has been proposed that these unique and developmentally regulated ESVs are the equivalent of a eukaryotic Golgi, as ESV's are responsible for the packaging and transport of cyst wall protein components to the cell periphery during encystation [17, 58].

Here we aim to investigate the role of *Gd* PITP through the utilisation of a highly characterised yeast PITP, Sec14p. Sec14p is a highly characterised PITP, and is utilised as a model for studies involving the characterisation of PITPs.

3.3 Results

3.3.1 *G. duodenalis* encodes for a single putative PITP

Given that PITPs are an essential and highly conserved eukaryotic protein family, investigation into its role in *G. duodenalis* may elucidate its novel role in encystation. The *G. duodenalis* genome has been annotated and found to encode for a single putative PITP gene (referred to as *Gd* PITP herein) (Figure 3.1). Work previously performed by a former lab member, determined the stage specific induction of *Gd* PITP at the mRNA level during encystation (Figure S1). Given these results, we further investigate *Gd* PITP and its role during encystation. Investigation into *Gd* PITP has seen that it is homologous to the classical PITP, mammalian PITPα (Figure 3.2), the prototypic StART-like PITP found throughout metazoa. The alignment of both *Gd* PITP and mammalian PITPα shows that the essential residues required for PtdIns binding (Thr^{59}, Lys^{61}, Glu^{86}, Asn^{90}, Thr^{114}) in PITPα to be conserved in *Gd* PITP in both *Gd* PITP A and *Gd* PITP B (Figure 3.2) [45]. As previously discussed, classical PITPs bind to PtdIns as well as PtdCho, though, intriguingly, the essential PtdCho

binding residues in PITPα are not conserved in either *Gd* PITP A or *Gd* PITP B. This suggests that the *Giardia* genome encodes for a single non-classical PITP that binds to PtdIns and a counter-ligand that is not PtdCho.

A phylogenetic analysis performed by Wyckoff and co-workers [59] has found the PITP family of proteins to represent a large but highly divergent family of proteins. In this study the PITPα protein sequence from *Rattus norvegicus* was used for a BLAST search to identify close and distant protein relatives. BLAST produced very weak alignments, even when numerous standard conditions were used. Sequence motifs appeared in some classes but not others thus rendering standard alignment and analysis methods ineffective. To circumvent this protein sequences were further analysed using MEME software [59] which identifies conserved sequence motifs in proteins based on the probability of the occurrence of an amino acid sequence in a motif derived from previous occurrences.

This study groups sequences from protists, including *Giardia duodenalis*, into a group that represents an ancestral group of PITP-like proteins [59]. Importantly this group provides the root of the phylogenetic tree, corresponding to the oldest point in the tree and gives evolutionary directionality to the tree. Key PtdIns binding residues, Thr 59 and Lys 61 in particular, are present in motifs found in all sequences studied to date, further emphasing that PtdIns binding is a critical function of PITPs conserved throughout evolution. Furthermore, phylogenetic analysis based on the presence or absence of conserved sequence motifs has suggested that the function or regulation of proteins in this family has changed dramatically, and is indicative of the type of specific adaptation often seen within protein families. It is likely that the identity of the PtdIns counter ligand changed to allow protein function adapt to the changing functional need of this family of proteins.

GL50803_4197 (PITP A)

ATGCGCTACTATGTGTTTGCCATCCCTCTCCCCTTCTCTATCGAGAAGTACAAGCTT
GGTCAGCTCTACATGGTCGCCAGGTCTACCCTAGAAGAGAGCTCCAAAAAGTCTTCT
GACGGATTTGAGATTCTTAAAAATGAACCGTACACCCGCACACTTCCTTCGGGACAG
GAGGAGTCTGGTATTTATACCTTTAAAATACTTCACTTGTCCAAAATGGTCCCCAAG
GCTGTTGCAAACCTTATTCCCAAGAAGGGTCTCAAGATGGAGGAGACCTGCTACAAC
GCTTTTCCCCACACAATAACATCGTATCACAACCCAGGGTATCCTGACAAGTTGGCA
ATGTCGGTCGAGACATGGGTCTACAGCGCACCAAAGAATGCGTCCTATTCCGAGGCC
TTTGATCTTCCTGAGGACGTTCGCAAGTGTATACCAGAATCATTCACTCTTGAGAAA
AAGGATAAAGAGTCGATGAAGAAGGATAAAGAGGCTCTTAAAGAGCGCAAAGACACA
GAGGATATATCGAAGCTAGAGTTTGCCGAGGCCAAAGGAGGTGTGATAGAACGAGTG
TACTGCGATGTCACGCAGCCTCTAAAGATAGACAAGAAAAAAGAAGCCAAGGAGAAG
AAACTCGCTGCTAAGGAGAACAGGGAGGCGCCGAAGGCTCTCAGCGAAGGTCCCTTG
AAGGCAGACATCAAGCGCATATCCAAAGAGAACAACGGTGACCACTGTGTAGTCTAT
AAGATCCTGAAGATCCATACTGCTTTTCCAGGCGAGAAACTTATCGAAAGCATGTTA
GGCAAGAAGATGGAATCAGTATTCACAGAAACACACAAGAAGTGCTGCATCTGGTGG
GACGAATGGAAGGAGATGACCATGGACGACATAAAGAAGATGGAAACTGACGCTGCA
GAGAAGCTGAAGAAGAGTATCGCTGAACGCGAGGCCGCAGGAAACGACTCCAAAGAA
ACGGAGTCCACTGGAGACGACGATGATGACGAGGTCGTCGAAGACGCAGACAAAGCT
GATGAAAAGTAA

MRYYVFAIPLPFSIEKYKLGQLYMVARSTLEESSKKSSDGFEILKNEPYTRTLPSGQ
EESGIYTFKLLHLSKMVPKAIANLIPKKGLKMEETCYNAFPHTVTSYHNPGYPDKLA
MSVETWVYSAPKNASYAETFDLPEEVRKSIPESFTLEKKDKESLKKDKEALKERKDT
EDISKLEFAEAKGGVIERVYCDVTQPLKIDKKKEAKEKKLAAKENREAPKALSEGPL
KADIKRISKENNGDHCIVYKILKVHTAFPGEKLIEGILGKKMESVFTETHKKCCIWW
DEWKGMTMDDIKKMENDAAEALKRTIAEREAANNDSKEEESTGDDDDDEVVEDADKA
DDK*

Figure 3.1A. nucleotide and amino acid sequence of *Gd* PITP A ORF. Highlighted in red are the targeted nucleotides for the production of the *Gd* PITP A^{T64D} mutant.

GL50581_3968 (PITP B)

ATGCGCTACTATGTGTTTGCCATCCCCCTTCCCTTCTCGATCGAGAAGTATAAACTC
GGGCAGCTCTACATGGTTGCCAGATCTACCTTAGAAGAGAGCTCCAAGAAGTCTTCT
GATGGGTTTGAGATTCTCAAAAATGAGCCGTACACTCGCACACTCCCCTCAGGACAG
GAGGAATCCGGCATCTATACCTTTAAGCTGCTTCACTTGTCCAAAATGGTACCCAAG
GCCATTGCAAATCTGATTCCCAAGAAGGGTCTCAAGATGGAGGAGACCTGTTACAAC
GCCTTCCCCCACACGGTTACGTCCTACCATAACCCCGGGTACCCCGATAAGCTGGCG
ATGTCGGTTGAGACCTGGGTCTATAGTGCTCCGAAGAACGCATCATACGCCGAGACC
TTCGACCTCCCCGAGGAGGTTCGCAAGAGTATACCGGAGTCATTTACTCTTGAGAAG
AAAGATAAGGAATCGCTGAAGAAGGACAAGGAGGCCCTTAAAGAGCGCAAAGATACA
GAGGATATTTCGAAGCTAGAGTTTGCAGAGGCCAAGGGGGGTGTCATCGAGCGTGTG
TATTGCGATGTCACACAGCCTCTGAAGATAGACAAGAAAAAGGAAGCTAAGGAGAAG
AAGCTTGCTGCCAAGGAGAACAGGGAAGCACCGAAGGCTCTCAGTGAGGGCCCTCTG
AAGGCAGACATTAAGCGTATCTCTAAGGAAAACAACGGCGACCATTGCATAGTCTAC
AAAATCCTGAAGGTCCATACGGCTTTTCCAGGCGAGAAGCTCATCGAAGGCATACTA
GGGAAGAAGATGGAGTCGGTGTTCACAGAAACACACAAGAAGTGCTGTATCTGGTGG
GATGAGTGGAAAGGAATGACTATGGATGACATCAAAAAGATGGAGAATGACGCGGCC
GAGGCCTTGAAGAGGACCATTGCGGAGCGCGAGGCAGCAAACAATGACTCCAAGGAA
GAAGAGTCCACTGGAGATGATGATGACGACGAAGTTGTCGAGGATGCCGATAAGGCC
GATGACAAGTGA

MRYYVFAIPLPFSIEKYKLGQLYMVARSTLEESSKKSSDGFEILKNEPYTRTLPSGQ
EESGIYTFKILHLSKMVPKAVANLIPKKGLKMEETCYNAFPHTITSYHNPGYPDKLA
MSVETWVYSAPKNASYSEAFDLPEDVRKCIPESFTLEKKDKESMKKDKEALKERKDT
EDISKLEFAEAKGGVIERVYCDVTQPLKIDKKKEAKEKKLAAKENREAPKALSEGPL
KADIKRISKENNGDHCVVYKILKIHTAFPGEKLIESMLGKKMESVFTETHKKCCIWW
DEWKEMTMDDIKKMETDAAEKLKKSIAEREAAGNDSKETESTGDDDDDEVVEDADKA
DEK*

Figure 3.1B. nucleotide and amino sequence of *Gd* PITP B ORF. Highlighted in red are the targeted nucleotides for the production of the *Gd* PITP B^{T64D} mutant.

Figure 3.2. Alignment of human PITPα and *G. duodenalis* PITP assemblage A and B. Critical PtdIns binding residues highlighted in black. T59 (human) and T64 (*G. duodenalis*) and the critical binding restudies for PtdCho in red. Residues identified by [45] and alignment performed using NCBI

3.3.2 *Gd* PITP is detrimental to *sec14-1ts* and *pik1-101ts*

The yeast protein Sec14p encoded by the essential *SEC14* gene is the prototypic PITP and the utilisation of the temperature sensitive mutant allele of Sec14p, *sec14-1ts*, has facilitated our understanding of PITP activity in other organisms. Previous studies have shown that the heterologous expression of mammalian PITPα was able to suppress this temperature sensitive growth defect of *sec14-1ts*. In contrast, expression of the PITPα^{T64D} mutant, a mutation known to disrupt the PtdIns binding activity of the PITP was unable to supress this growth defect [45]. This then lead to investigate whether *Gd* PITP could suppress *sec14-1ts* growth defects.

To investigate the effects of *Gd* PITP on *sec14-1ts*, a yeast expression vector was constructed utilising the pDR195 expression vector. As mentioned, the critical PtdIns binding residues are conserved in both *Gd* PITP A and *Gd* PITP B. Sequence alignment using Clustal Omega software identifies the amino acid Thr 64 as a critical PtdIns binding residue present in both PITPs Figure S1. To obtain a PtdIns binding mutant, site-directed mutagenesis was performed whereby Thr 64 in *Gd* PITP A and *Gd* PITP B was mutated to an Aspartate (Asp/D), a mutation which inhibits PtdIns binding. From here, the *Gd* PITP open reading frame (ORF) from both *G. duodenalis* assemblage A and B along with their T64D mutated ORF (Figure 3.3A,B) were cloned using the restriction sites of *XhoI* and *BamHI* (Figure 3.3C) and placed under the transcriptional control of the yeast *PMA1* promotor (Figure 3.3A/B). These expression vectors were utilised in this study for the investigation into *Gd* PITP on yeast *ts* mutants. When investigating the function of PITPs, a PITP that enables growth of *sec14-1ts* not only at the permissive temperature of 30°C but also at the semi and non-permissive temperatures of 34 - 37°C respectively are routinely classical PITPs, although exceptions do exist. In contrast, PITPs that do not allow growth at the semi and non-permissive temperatures are non-classical PITPs, though the non-classical PITPs typically allow growth at the non-permissive 30°C.

Contrary to what was observed with the mammalian PITPα expression in *sec14-1ts*, we observed that heterologous expression of *Gd* PITP A and *Gd* PITP B was in fact detrimental to the growth of *sec14-1ts* (Figure 3.4). This detrimental effect was even observed at the permissive temperature (30°C) as little cell growth was observed at

this temperature. (Figure 3.4). Interestingly, the growth of *sec14-ts* mutants was unaffected by heterologous expression of either *Gd* PITP A^{T64D} and *Gd* PITP B^{T64D} PtdIns binding mutants.

Sec14p functions by presenting PtdIns to the PtdIns-4-OH kinase (Pik1p) to facilitate PtdIns-4-P synthesis. Given the observation that heterologous expression of *Gd* PITP A and *Gd* PITP B is detrimental to growth of *sec14-1ts,* we were interested in investigating if heterologous expression of either *Gd* PITP A or *Gd* PITP B also exacerbated the growth defect of the *ts PIK1* mutant, *pik1-101ts*. Interestingly, the growth profile of *pik1-101ts* mutants expressing either *Gd* PITP A or *Gd* PITP B completely phenocopied that of *sec14-1ts.* That is, heterologous expression of either *Gd* PITP A or *Gd* PITP B was detrimental to the growth of *pik1-101ts* but the expression of the PtdIns binding mutant, *Gd* PITP A^{T64D} and *Gd* PITP B^{T64D} was not and allowed growth at the permissive temperature (Figure 3.4).

To rule out whether the overexpression of either *Gd* PITP A or *Gd* PITP B was toxic to cell growth, the growth of wildtype cells, BY4742, expressing these genes was investigated. The growth of wild type cells observed that they were not affected by the overexpression of these genes (Figure 3.4).

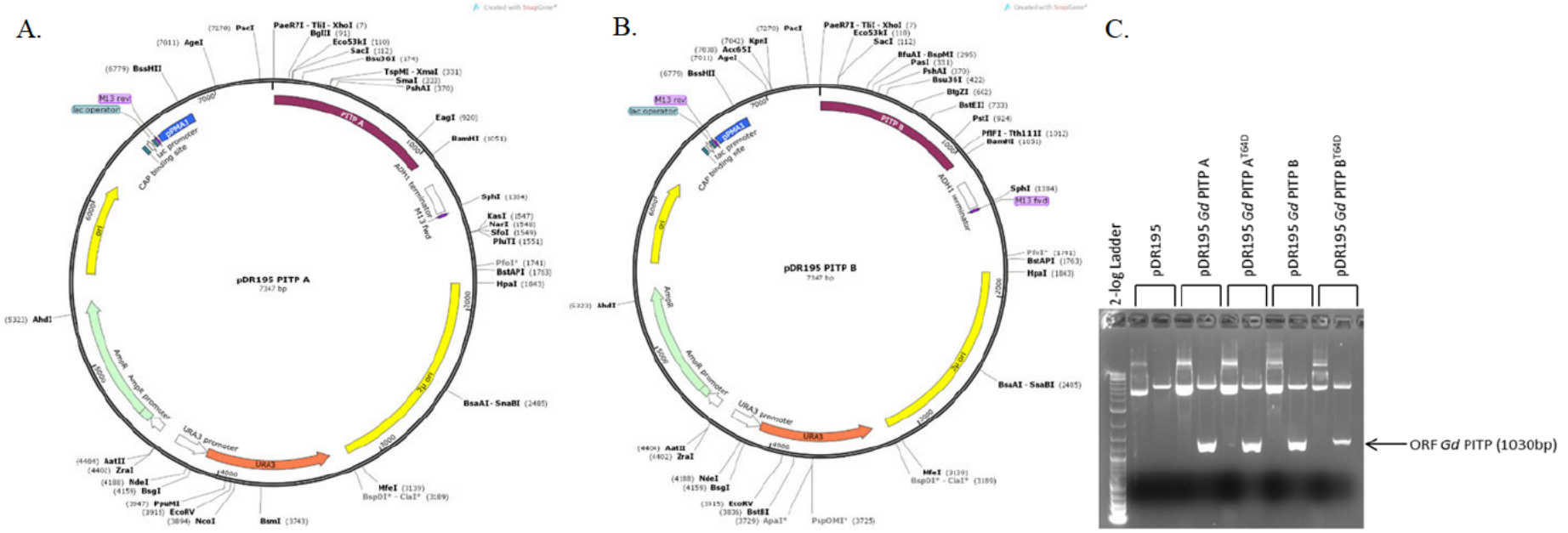

Figure 3.3. Vector map of the yeast expression vector pDR195 whereby the **A.** *Gd* PITP A/A^{T64D} ORF is placed under transcriptional control of *PMA1* with a uracil selectable gene. **B.** *Gd* PITP B/B^{T64D} ORF is placed under transcriptional control of *PMA1* with a uracil selectable gene. **C**. Restriction endonuclease digest (*XhoI* and *BamHI*) of the ORF showing *Gd* PITP derivatives in the pDR195 yeast expression vector utilised for further experiments.

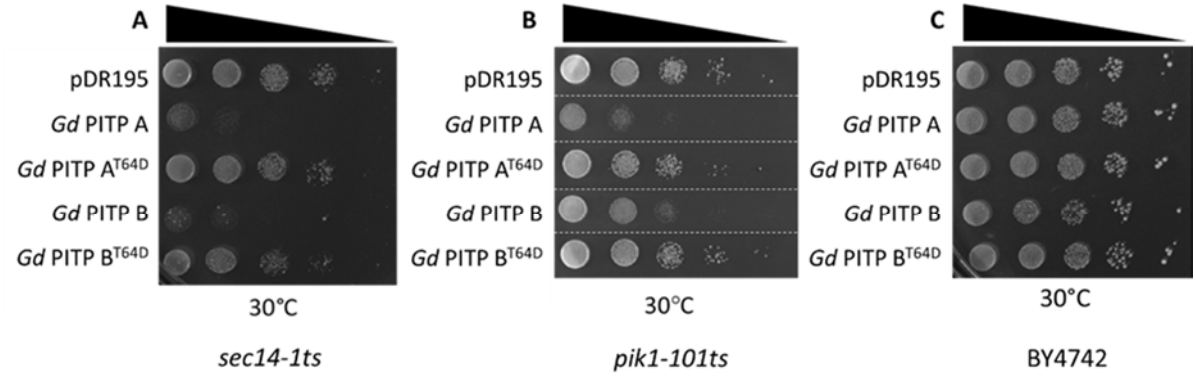

Figure 3.4. Serial-spot dilutions (neat, 1/10, 1/100, 1/1000, 1/10 000) **A.** *sec14-1ts*, **B.** *pik1-101ts* and **C.** BY4742 cells expressing vector control pDR195, *Gd* PITP A, *Gd* PITP A^{T64D}, *Gd* PITP B, *Gd* PITP B^{T64D} at 30°C

3.3.3 *Gd* PITP alters neutral lipid metabolism

The effect of *Gd* PITP A and *Gd* PITP B on the growth of the temperature sensitive mutants *sec14-1ts* and *pik1-101ts* is reminiscent of what was observed upon heterologous expression of a different yeast PITP *SFH3*[53]. Overexpression of *SFH3* exacerbated the growth defect of both *sec14-1ts* and *pik1-101ts*. In the context of Sfh3p, this was due to the redirection of essential PtdIns-4-P production in the *trans* Golgi-network to lipid droplets (LD) a non-essential process, preventing the breakdown of neutral lipids in these storage organelles [48, 53]. This was concluded as neutral lipid turnover was strongly diminished in both *sec14-1ts* and *pik1-101ts* cells overexpressing *SFH3* but not a PtdIns binding mutant. Given what is known and observed with *SFH3* we questioned whether heterologous expression of *Gd* PITP A or *Gd* PITP B had a similar effect on LD dynamics.

This was tested by investigating the LD content within the *sec14-1ts* cells overexpressing *Gd* PITP A and *Gd* PITP A^{T64D}. We chose to use only *Gd* PITP A (WT and A^{T64D}) for these experiments since *Gd* PITP A and *Gd* PITP B (which have high sequence identity, Figure 3.2) behaved similarly in the growth assay (Figure 3.4).

These cells were stained with BODIPY™ 493/503 to allow for staining of neutral lipid such as triacylglycerols (TAGs) and sterol esters found within LD. The fluorescent intensity of these cells was measured using flow cytometry, and the number of lipid droplets visualised using fluorescent microscopy. *Gd* PITP A (but not *Gd* PITP B)

Flow cytometry indicated that cells overexpressing *Gd* PITP A had a higher median fluorescent intensity (MFI) compared to cells containing the vector control, pDR195, representing the cells in a wild-type manner indicative of a higher neutral lipid content (Figure S2). Cells overexpressing the PtdIns mutant *Gd* PITP A^{T64D} measured a lower MFI compared to that of *Gd* PITP A and a similar MFI to that of the vector control, indicative of a lower lipid content to that of *Gd* PITP A (Figure S2). This suggests that overexpression of *Gd* PITP A results in cells possessing elevated levels of neutral lipids.

To further validate the flow cytometry results and to have a visual representation of the cells, fluorescent microscopy was performed with these same cells, *Gd* PITP A and *Gd* PITP A^{T64D} alongside the vector control. Validating our flow cytometry results,

fluorescent microscopy found results complementing that of Flow cytometry. *Sec14-1ts* cells overexpressing *Gd* PITP A saw a larger number of fluorescently stained neutral lipids with a higher intensity of fluorescence compared to vector control cells (approx. 1.6-fold) (Figure 3.5). Additionally, cells overexpression *Gd* PITP A^{T64D} saw a fewer number of fluorescently stained neutral lipids and overall, less intense fluorescence, similar to that of the vector control. This is indicative of less LD's in cells ever expressing *Gd* PITP A^{T64D} and vector control, compared to those over expressing *Gd* PITP A (Figure 3.5)

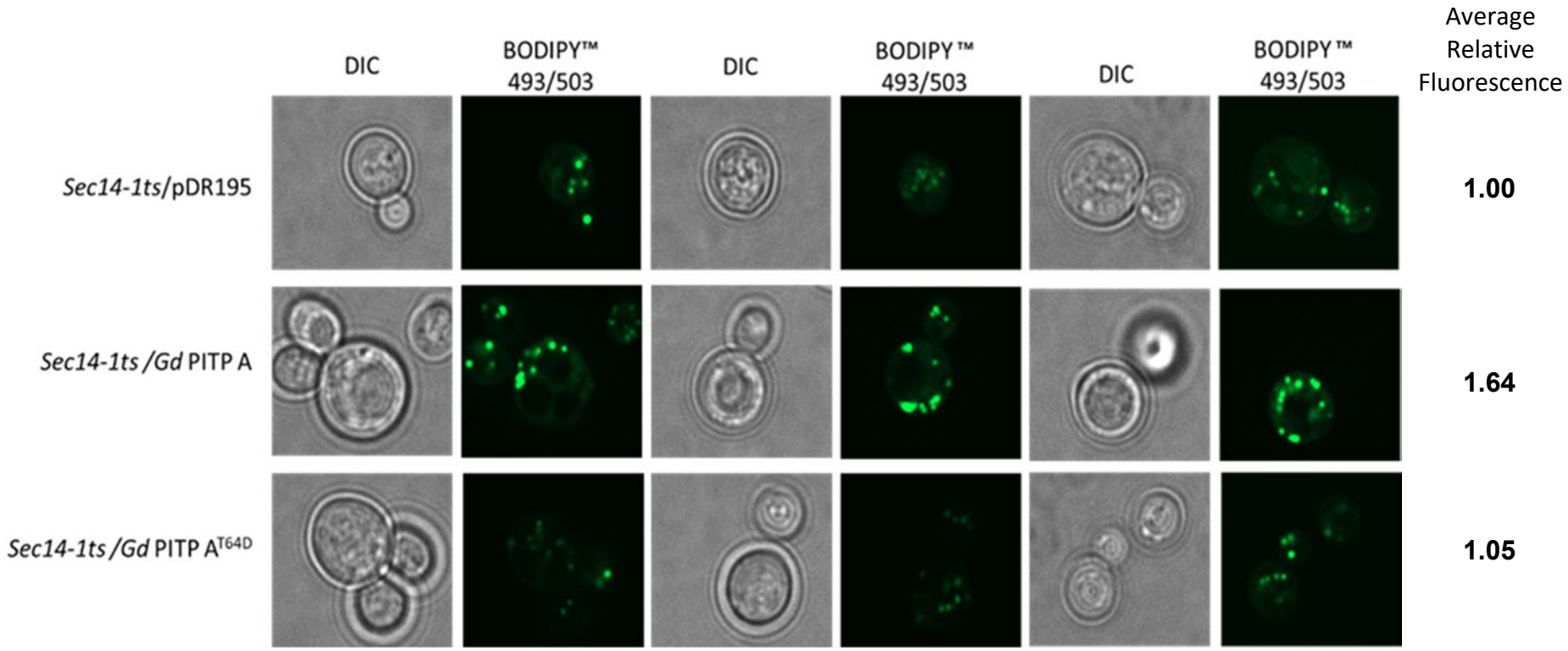

Figure 3.5. DIC and fluorescent microscopy images of *sec14-1ts* overexpressing pDR195, *Gd* PITP A and *Gd* PITP A^{T64D}. Cells observed were derived from the same population of cells utilised for the flow cytometry assay. Cells were stained with BODIPY™ 493/503, staining neutral lipids to allow for visualisation of GFP. The average relative fluorescence was determined in Image J. For this, an oval was drawn around the outline of each cell in each panel with the area of the oval and total fluorescence recorded. The relative fluorescence of a cell was determined by dividing the total fluorescence by the area of the oval and the average for each condition determined. The average relative fluorescence is shown relative to pDR195 control.

3.3.4 *Gd* PITP is hypersensitive to miconazole

Given the phenotypic similarities observed between Sfh3p and *Gd* PITP, we wanted to further investigate whether the phenotypic similarities could be translated further to mechanism of function. Given that Sfh3p is a PITP that binds to ergosterol, studies identified the specific hypersensitivity of *sfh3Δ* strain to azole drugs such as miconazole, that are inhibitors of ergosterol biosynthesis [53]. Studies have reported a specific phenotype with *sfh3Δ* whereby these mutants show hypersensitivity to sub lethal doses of miconazole ($\geq 0.1\mu g/mL$) but are more resistant to these drugs than WT cells at acute high-doses ($\leq 0.1\mu g/mL$) [53].

Given that *Gd* PITP is phenotypically similar to Sfh3 with regards to *sec14-1ts* and *pik1-101ts* cells we investigated whether *Gd* PITP phenocopied sfh3 in the context of miconazole hypersensitivity. For this, *Gd* PITP A, *Gd* PITP B and their derivatives were overexpressed in *sfh3Δ* cells and grown on media containing varying concentrations of miconazole at sub-lethal and growth was assessed compared to *SFH3*. Results from this experiment identified that *Gd* PITP possesses a higher sensitivity to miconazole compared to *SFH3* with reduced growth at 0.1 and 0.5µg/mL compared to *sfh3Δ* (Figure 3.6). In addition to this, the *Gd* PITP PtdIns mutants, *Gd* PITP A^{T64D} and *Gd* PITP B^{T64D} allowed growth in the presence of 0.1 and 0.5µg/mL miconazole therefore restoring this hypersensitivity to allow growth equal to that of vector control (Figure 3.6).

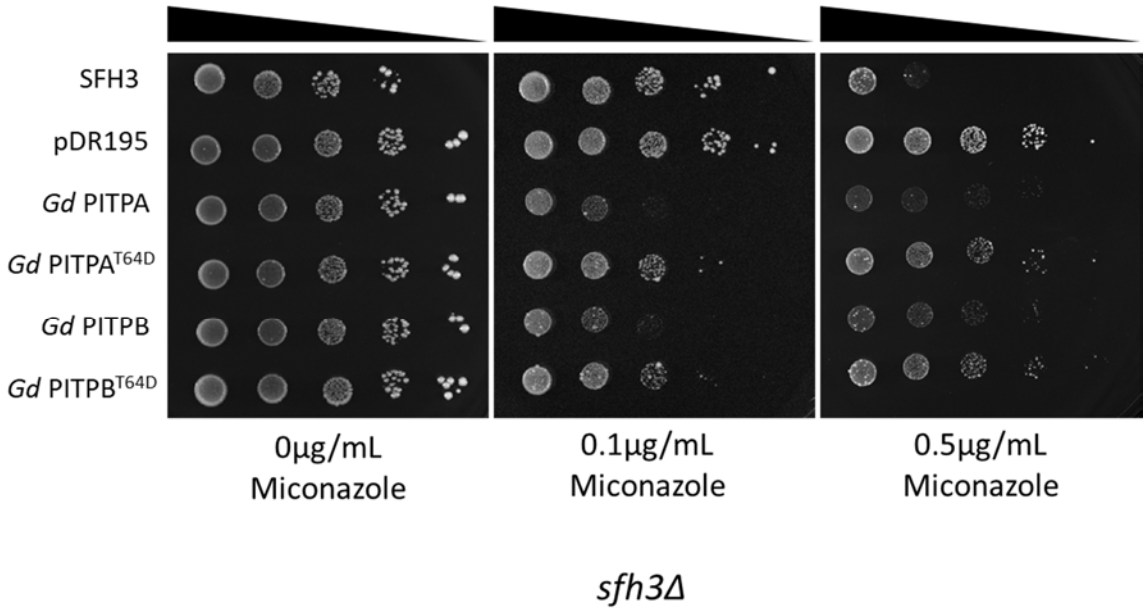

Figure 3.6 Serial-spot dilutions (neat, 1/10, 1/100, 1/1000, 1/10 000) of *sfh3Δ* cells over expressing SFH3, pDR195. *Gd* PITP A, *Gd* PITP A^{T64D}, *Gd* PITP B and *Gd* PITP B^{T64D} grown on plates containing 0, 0.1, and 0.5 µg/mL miconazole and grown at 30°C.

3.4 Discussion

Combining whole cell proteomic analysis of *G. duodenalis* performed by Faso *et al.,* 2013 along with bioinformatic analysis and previous gene expression data, we identified that *G. duodenalis* encodes for a single putative PITP with increased expression specifically during encystation, though to date, this protein is uncharacterised. Due to lack of knowledge surrounding *Gd* PITP, we therefore sought to characterise the function of *Gd* PITP.

To characterise *Gd* PITP, we analysed the role of PITPs in other organisms, in particular *S. cerevisiae*, which serves as a useful model due to its genetic tractability and its highly characterised nature of its PITPs such as Sec14p. Additionally, Sec14p and specifically the *ts* mutant *sec14-1ts* is a model utilised in early studies into PITP characterisation. This PITP promotes Golgi secretory function through the regulation of the lipid membrane composition [30, 35, 60, 61]. Interestingly, the results from the yeast spot-dilution assay above, revealed an unusual growth phenotype with the *ts* mutant. Rather than allowing these cells to grow at the permissive and non-permissive temperatures being suggestive of a classical PITP, or only allowing growth only at the permissive temperature, suggestive of a non-classical PITP, *Gd* PITP A and *Gd* PITP B exacerbated the growth of these *ts* cells. This growth phenotype has only been observed with regards to a specific PITP, Sfh3p. Sfh3p has recently been characterised as a PITP involved in process of sporulation, a response to nutrient stress [46, 48, 62] Sporulation, though a different to encystation possesses characteristics comparable to encystation in *G. duodenalis,* which is triggered by nutrient deprivation. Given that *Gd* PITP has been indicated to be upregulated during encystation and Sfh3p is a PITP specifically involved in sporulation, this poses the question to whether Gd PITP may be as important during encystation as sfh3p is to sporulation.

To investigate the role of *Gd* PITP and this unique phenotype, we utilised Sfh3p as a model for *Gd* PITP. In addition to the *sec14-1ts* mutants, the PtdIns-4-OH kinase *ts* mutant *pik1-101ts* was investigated as this exacerbated growth was observed in these cells, when Sfh3p was overexpressed in these cells. Expression of *SFH3* in these *ts* mutants was seen to be detrimental, with cells displaying little growth at permissive temperatures [53]. Much like Sfh3p, *Gd* PITP A and *Gd* PITP B showed the same

exacerbated growth as what was observed in *sec14-1ts* and therefore we used work performed on Sfh3p as a model for determining the function of *Gd* PITP. Further characterisation by Ren *et al.,* 2014 into Sfh3p determined that this exacerbated growth was due to the lipid environment within these cells as PITPs are responsible for the link between lipid metabolism and cellular functions. It was found that Sfh3p redirected an essential process of PtdIns-4-P production from the *trans* Golgi to a non-essential process in LD, preventing the breakdown of neutral lipids within the cell [48, 53]. Interestingly, when *Gd* PITP A and *Gd* PITP B was overexpressed in these same *ts* mutants, we observed growth reminiscent of *SFH3*. However, overexpression of the PtdIns binding mutants *Gd* PITP^{T64D}, enabled grow at the permissive temperature, suggesting this growth defect is due to PtdIns binding. Combining what we have observed with *Gd* PITP and with previous knowledge of Sfh3p, this data suggests that *Gd* PITP facilitates PtdIns binding in a Sfh3p dependant manner.

After investigating the effects of *Gd* PITP on the growth of *ts* cells we sought to investigate the lipid environment of these cells as it is hypothesised that *Gd* PITP may be acting in a Sfh3p manner, altering the lipid environment. This was investigated through two processes, flow cytometry to investigate the cell population and fluorescent microscopy to visualise the lipid environment of these same cells. Results from these experiments suggested that *Gd* PITP affects the lipid droplet metabolism of the cell in a PtdIns dependant manner. This is hypothesised as *sec14-1ts* cells overexpressing *Gd* PITP A saw a larger number of cells with a higher MFI compared to that of both vector control and *Gd* PITP^{T64D} the mutant with ablated PtdIns binding. Interestingly, in addition to the differences in median fluorescence intensity (MFI), a difference in population distribution was observed. The *Gd* PITP A population appeared to be unimodal whereas in comparison the *Gd* PITP A^{T64D} population appeared bimodal. This bimodal appearance may be representative of a heterogeneous population of cells, with some containing a higher level of lipid than others, whereas the unimodal population may be representative of a cell population containing a high percentage of cells with a higher lipid content.

Additionally, the fluorescent microscopy further clarified our suspicions on the lipid environment of the cell where *sec14-1ts* cells over expressing *Gd* PITP A possessed a larger number of visibly stained neutral lipids. In contrast, *Gd* PITP A^{T64D} and vector control contained some cells with brighter stained lipids while others had fewer and

fainter droplets. This finding helped to explain the unimodal and bimodal appearance of *Gd* PITP A and *Gd* PITP A^{T64D} , respectively, in the flow cytometry results. In confirmation of our findings, similar techniques undertaken in previous studies performed with Sfh3p detailed a cellular environment with a larger accumulation of neutral lipids compared to that of wild-type cells [53]. Given that *Gd* PITP is affecting growth of these *ts* cells in a similar way to Sfh3p, we hypothesised that it may be altering the lipid environment of these cells through a similar activity.

To further validate our findings that the *Gd* PITP is a Sfh3p-like PITP, we investigated the function of *Gd* PITP in the context of sterol synthesis. This was previously investigated with regards to Sfh3p, a sterol binding protein, through the use of a miconazole sensitivity assay. This assay can be used to investigate sterol synthesis where sensitivity to miconazole can be an indication of altered sterol synthesis. When this assay was performed with Sfh3p, cells showed a unique phenotype where they were seen to be hypersensitive to miconazole at sublethal doses of 0.1 and 0.5µg/mL yet these cells are more resistant to miconazole than WT cells at acute high doses. A study observing this, hypothesised that this unique phenotype was related to an accelerated depletion in LD reserves [53]. Given the similarities observed with *Gd* PITP and Sfh3p with regards to *sec14-101ts* and *pik1-101ts* cells, we wanted investigate whether *Gd* PITP observed similar hypersensitivity to miconazole as Sfh3p. Interestingly results from the miconazole sensitivity assay showed that not only was *Gd* PITP hypersensitive to miconazole at these same sub-lethal doses, but *Gd* PITP was seen to be more hypersensitive to miconazole than Sfh3p with a reduced growth compared to Sfh3p, suggesting that *Gd* PITP may intersect with neutral lipid metabolism more effectively than Sfh3p-like PITP. Given these results, this is suggestive that *Gd* PITP may be a PITP involved in sterol synthesis. Furthermore, growth of the PtdIns binding mutants *Gd* $PITP^{T64D}$ allows cells to grow at these miconazole levels therefore restoring this hypersensitivity to this drug. Given our understanding of PITPs and their function, using the counter-ligand exchange, this suggests that miconazole hypersensitivity is a result of the activity of a functional *Gd* PITP. On the contrary, this hypersensitivity is not seen in the non-functional PtdIns binding mutants *Gd* $PITP^{T64D}$, further confirming that this phenotype is observed due to the activity of the functional *Gd* PITP.

Several studies have elucidated the novel role of Sfh3p in PtdIns binding and lipid droplet metabolism and its consequent impact on the formation of spores in response to nutrient stress. Data presented herein is reminiscent of what was observed with Sfh3p and strongly suggests the notion that *Gd* PITP may possess a similar activity to Sfh3p in the context of encystation.

Chapter 4

Characterisation of *Gd* PITP lipid binding activity

4.1 Introduction

PITPs are an ancient protein superfamily and are present in all eukaryotes and facilitate membrane trafficking and signalling though the coordination of PIPs [40]. PITPs bind to PtdIns as well as a counter ligand. This counter ligand can be a lipid such as PtdCho or a lipophilic molecule. PITPs and are broken down into two major groups, the Sec14-PITPs and the StART-like PITPs. These groups are structurally dissimilar though share the ability to bind PtdIns [63]. Furthermore, these families can be broken into the 'classical' PITPs, characterised by their ability to bind to PtdIns and PtdCho. The other major group are the 'non-classical' PITPs, characterised by their ability to bind to PtdIns and a different counter ligand [36, 47, 49, 61]. All StART-like PITPs, to date, have been classified as classical [47] though new StART-like PITP candidates are emerging and may elucidate the presence of StART-like PITPs in ancient eukaryotes [63]. PITPs are proposed to function via two non-mutually exclusive mechanisms. Originally, it was proposed that PITPs function as a classical lipid transport protein, allowing the transfer of lipids from a high concentration to a low concentration to facilitate the generation of specialised lipid environments within the cell [64]. The other proposed mechanism and the method that we are most interested in is for the formation of vesicles. Here the PITP presents PtdIns to the PtdIns-4-OH kinase Pik1p. PtdIns is then phosphorylated at the 4' hydroxyl where PtdIns-4-P is produced and imbedded into the lipid membrane. As the concentration of PtdIns-4-P increases within the membrane, co-proteins are recruited to enable the destabilisation of the membrane forming a bud. Eventually the bud breaks away from the lipid membrane and a vesicle is produced [32, 65].

Bioinformatic analysis of the *G. duodenalis* genome identified a single putative PITP, *Gd* PITP. To date, nothing is known about this *Gd* PITP, however, alignment of *Gd* PITP against its closest homologue, mammalian PITPα identified that the critical binding residues for PtdIns binding were conserved in *Gd* PITP A and *Gd* PITP B. The critical binding residues required for PtdCho were not conserved in *Gd* PITP A and *Gd* PITP B suggesting that *Gd* PITP is a 'non-classical' PITP. Work performed on *Gd* PITP revealed an intriguing growth phenotype reminiscent of a specific PITP, Sfh3p. Sfh3p is a non-classical PITP, involved specifically in sporulation, a stress response in *S. cerevisiae*. Sporulation, like encystation, is a stress response due to nutrient and

environmental stress and these processes can be comparable. Furthermore, Sfh3p has recently been characterised as a non-classical PITP, binding to sterol.

Whilst it is hypothesised that *Gd* PITP is a non-classical PITP crucial for the developmental process of encystation, the lipid binding properties of *Gd* PITP have yet to be determined. To fill this gap of knowledge, we sought to determine the lipid binding activity of *Gd* PITP that may elucidate its importance during encystation.

4.2 Results

4.2.1 Recombinant *Gd* PITP protein expression in *E. coli*

Functionally, PITPs are classified as being either 'classical' or 'non-classical' defined by their binding activity. Typically, the characterisation of a PITP begins with investigation into whether they enable *sec14-1ts* to grow at 34-37°C. Classical PITPs allow growth at these temperatures while non-classical do not. Interestingly *Gd* PITP revealed a severe non-classical phenotype with no growth at 34-37°C as well as an exacerbation of the growth phenotype at 30°C. Given that our preliminary characterisation suggests that *Gd* PITP is likely a non-classical PITP, we wanted to investigate its activity further. To investigate this, we required the expression and purification of epitope tagged recombinant protein of *Gd* PITP A and *Gd* PITP B as well as the PtdIns binging mutants *Gd* PITP A^{T64D} *Gd* PITP B^{T64D} from *E. coli*.

The open reading frame of *Gd* PITP A and *Gd* PITP B along with their corresponding T64D mutants were cloned by PCR using oligonucleotides in which the forward and reverse were clamped with *NdeI* and *BamHI* restriction sites, respectively. After restriction digest (Figure 4.1), the fragment was ligated into the pET16B *E.coli* expression vector giving pET16b-*Gd* PITP A, pET16b-*Gd* PITP B, pET16b-*Gd* PITP A^{T64D}, pET16b-*Gd* PITP B^{T64D} (Figure 4.1B).

The BL21 DE3 system enables high level expression of recombinant protein upon incubation with IPTG. Induced expression in BL21 DE3 cells stem from T7 RNA polymerase bring integrated into the *E. coli* genome under transcriptional control of the Lac operon. Incubation with IPTG induces expression of T7 RNA polymerase

which in turn induces expression of the recombinant gene placed downstream of the T7 promotor (Figure 4.1). An induction profile was conducted to verify that expression of 10xHis-*Gd* PITP A, 10xHis *Gd* PITP B (and their mutant derivatives) could be induced. Robust protein expression is observed in all proteins after two hours post induction with IPTG (Figure 4.2A). Importantly, the PtdIns binding mutants, T64D has no effect on protein stability, as yield is comparable. His-tagged protein was confirmed via immunoblotting at the expected 39kDa (Figure 4.2B).

4.2.1 Purification of *Gd*PITP derivatives

Following on from confirmed protein derivates, these will be used in lipid binding assays that required the input protein to be soluble and stable. Therefore, these recombinant proteins must be purified from the soluble fraction of a cell lysate and not inclusion bodies. A small-scale induction was performed, and cell lysates fractionated into a 15 000g supernatant (soluble fraction) and pellet (insoluble fraction) to determine that a suitable amount of recombinant protein remains soluble for future assays. This small-scale induction confirmed that there was suitable soluble protein present for the continuation of this experiment (Figure 4.3). However, a significant proportion of purified protein was in the insoluble fraction. We hypothesize this is due to the robust expression of the protein leading to the formation of protein aggregates.

With confirmation of induced soluble protein, protein inductions were scaled up to allow for larger quantities of protein for purification. Cultures of these proteins were grown in 400 mL of LB in culture flasks and induced with IPTG and incubated overnight Following induction, these cells were purified via His purification as outlined in the methods (section 2.15 Purification of polyhistidine tagged protein) (Figure 4.4) and the used in future assays.

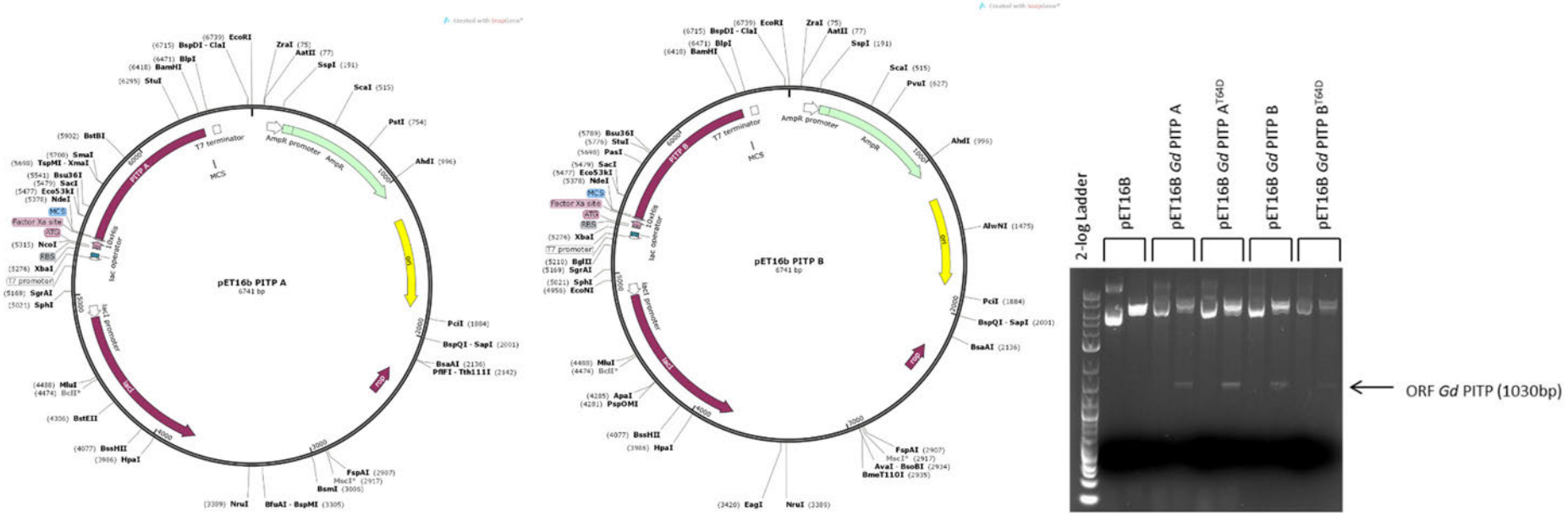

Figure 4.1 Vector map of the *E. coli* expression vector pET16b whereby the A. *Gd* PITP A/A^{T64D} ORF is N-terminally 10x His tagged placed under transcriptional control of T7 promotor with an Ampicillin resistance selectable gene. B. *Gd* PITP B/B^{T64D} ORF is N-terminally 10x His tagged placed under transcriptional control of T7 promotor with an Ampicillin resistance selectable gene. C. Restriction enzyme digest (*XhoI* and *NcoI*) of the ORF of *Gd* PITP derivatives from the pET16b.

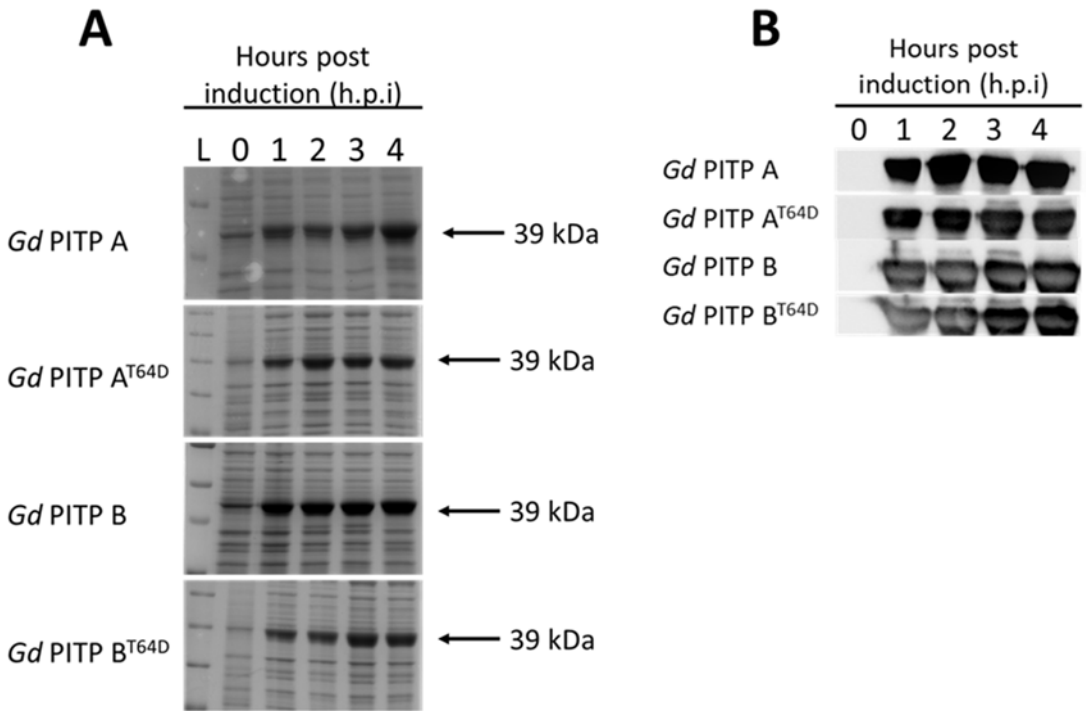

Figure 4.2. Induction profile of *Gd* PITP derivatives in the form of A. SDS-Page stained with Coomassie to stain total protein content and B. Immunoblot of 10xHis tagged *Gd* PITP

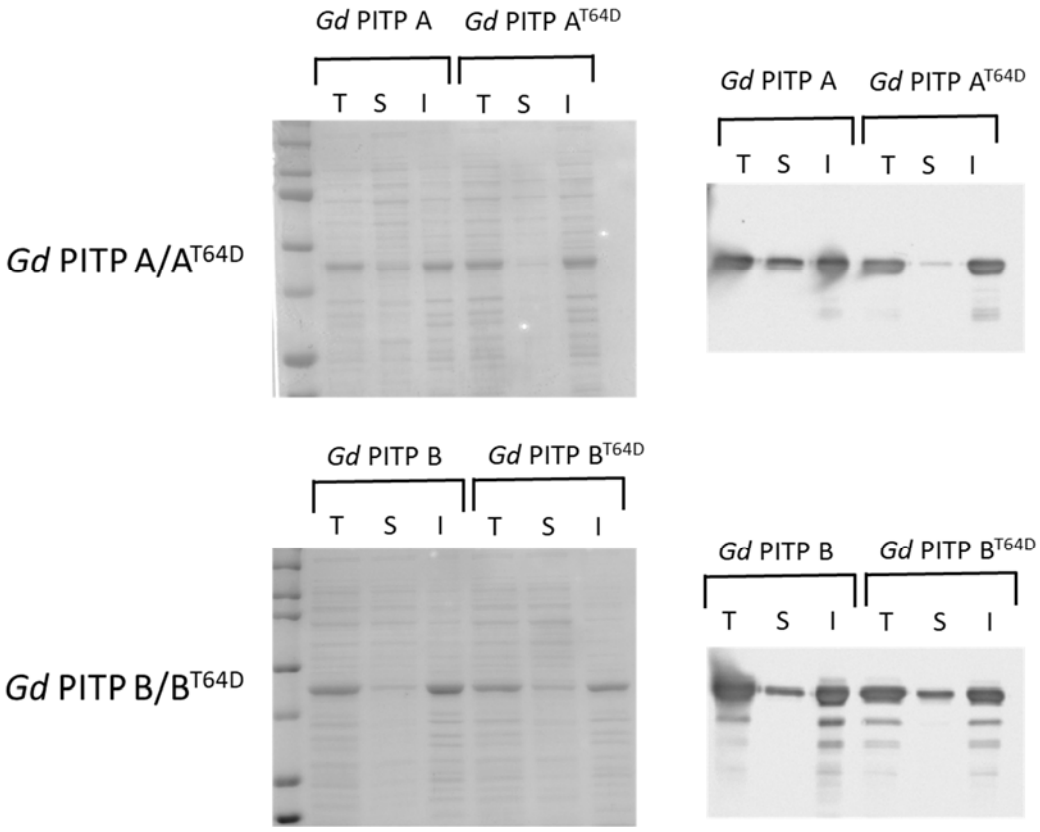

Figure 4.3 Coomassie and immunoblot of *Gd* PITP A, Gd PITP B and their mutants fractionated into total protein (T), soluble (S) and insoluble (I) fractions.

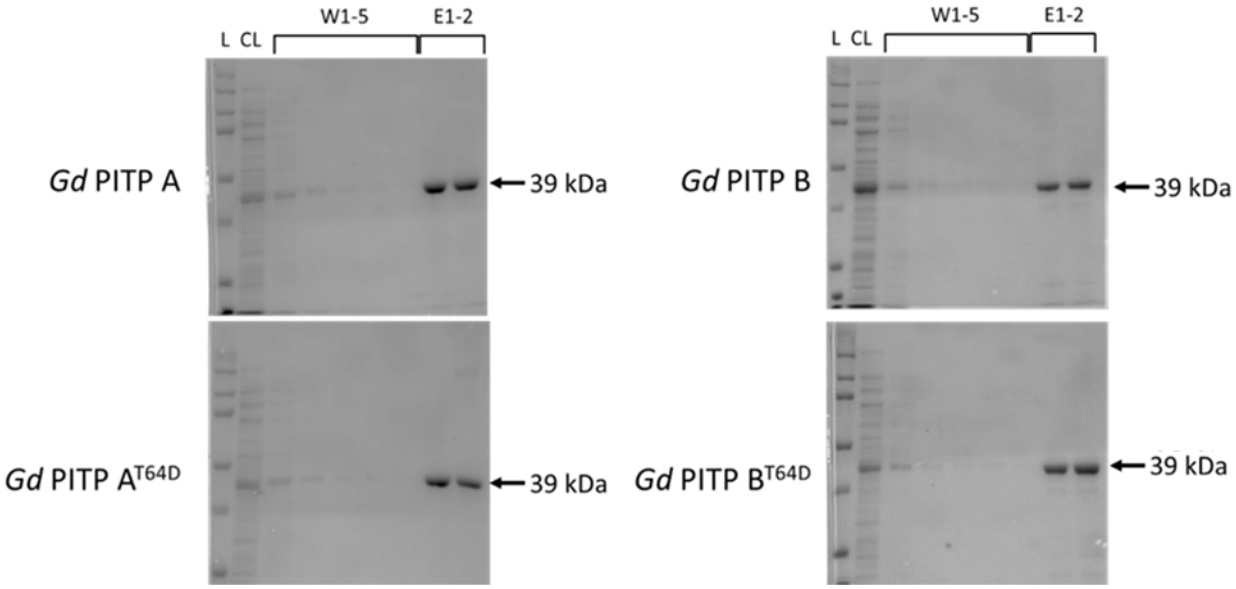

Figure 4.4. His purification fractions of *Gd* PITP and derivatives including cell lysate (CL), Washes 1-5 (W1-5) and elution's (E1-2).

4.2.2 Lipid Binding Assay

As previously mentioned, cholesterol is an integral part of the *G. duodenalis* lifecycle. If cholesterol is unavailable, *G. duodenalis* is triggered to follow down a developmental pathway leading to a metabolically inert, environmentally resistant form, the cyst [1, 3, 21, 24]. Given that cholesterol is so important in the lifecycle of *G. duodenalis*, we wanted to investigate whether this lipid may be the counter ligand for *G. duodenalis* given that it possessed characteristics of a non-classical PITP.

To determine the lipid binding properties of *Gd* PITP, a targeted approach was undertaken in which *Gd* PITP A and *Gd* PITP B were incubated with fluorescently labelled cholesterol (TopFluor®) (Figure 4.4), enabling the determination of its cholesterol binding activity. This experiment utilised Kes1p as a positive control, a sterol binding protein. This protein has been utilised in other experiments as the gold standard sterol binding protein. Additionally, two negative controls were utilised for this experiment. Sec14p, a classical PITP unable to bind to sterol as well as a mutated derivative of Kes1p, $Kes1^{Y97F}$, a mutation shown to ablate sterol binding. These proteins were purified via His-purification (Figure 4.5) and were run alongside each other in triplicate and results were determined using the Perkin Elmer™ Ensight plate reader and Fluorescence Intensity Units (FIU).

Results from this assay determined that there was little to no significant difference of the cholesterol binding between each protein, with FIU slightly above that of background and significantly below the expected binding for Kes1p (Figure 4.6). Therefore, suggestive that no protein was bound to more cholesterol over another.

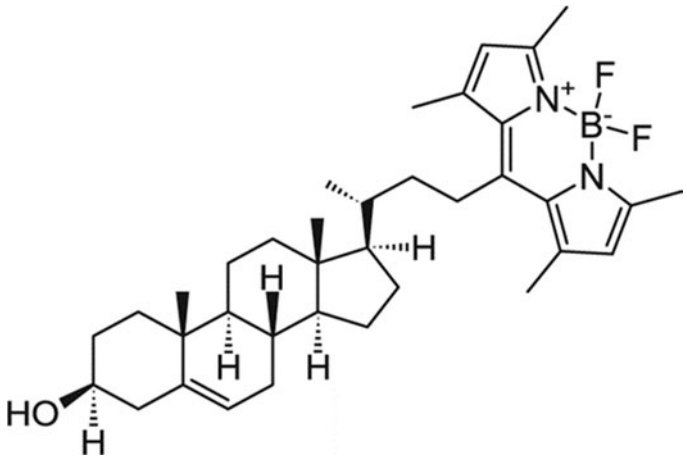

Figure 4.5. Structure of TopFluor® cholesterol from Avanti® Polar Lipids Inc.

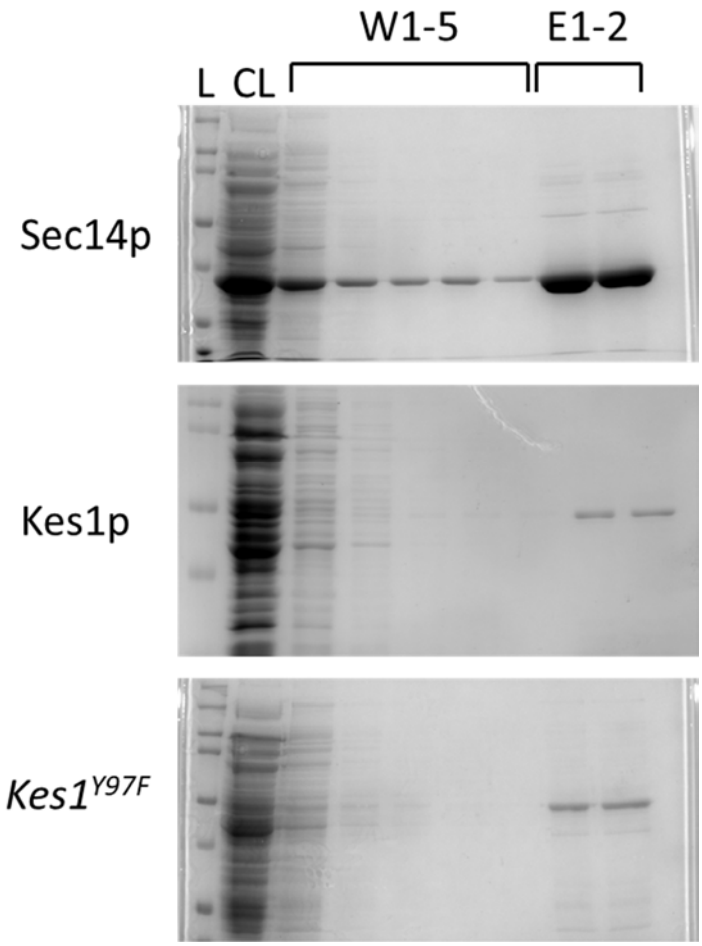

Figure 4.6. His purification fractions of the control proteins used in the lipid binding assay Sec14p, Kes1p and *Kes1*^{Y97F} including cell lysate (CL), Washes 1-5 (W1-5) and elution's (E1-2).

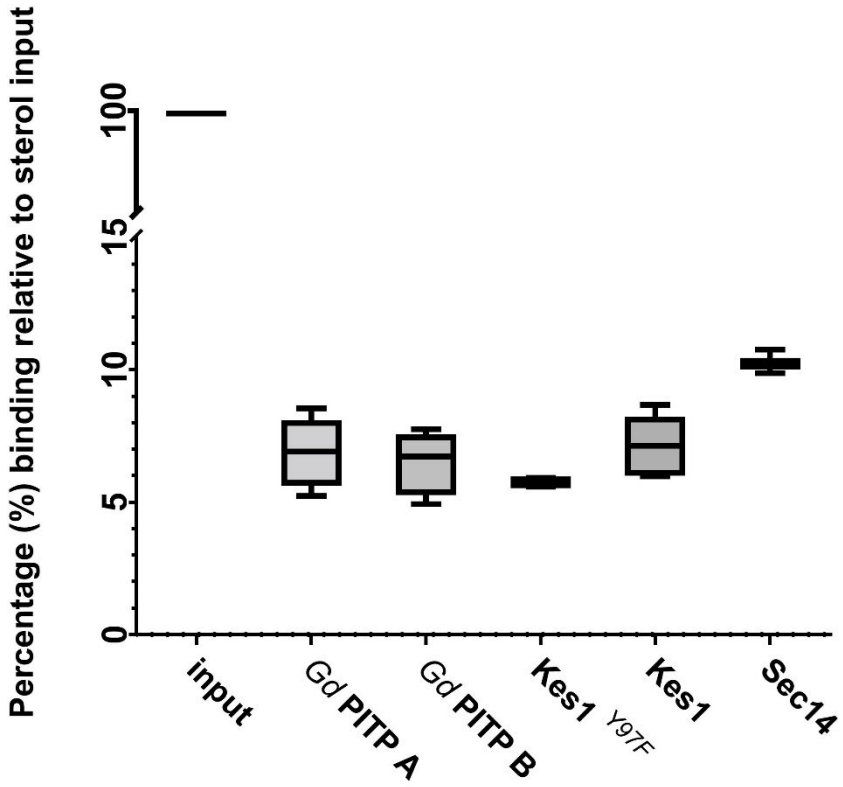

Figure 4.7. Box and whisker plot representing percentage (%) binding of *Gd* PITP A, *Gd* PITP B, Kes1, *Kes1*^{Y97F} and Sec14 relative the input of TopFluor®

4.2.3 Lipidomics - Mass Spectroscopy

Along with a targeted approach, a non-targeted approach was utilised to determine the counter ligand of *Gd* PITP. This was performed by incubating *Gd* PITP with lipids extracted with methanol chloroform from *S. cerevisiae* wild-type cells, BY4742. The recombinant purified *Gd* PITP derivatives were incubated with these lipid extracts and purified via metal^{2+} affinity chromatography. *Gd* PITP A and *Gd* PITP B will be used as a PtdIns binding control as it is predicted that *Gd* PITP has a preferential affinity to bind to PtdIns. The PtdIns binding mutants *Gd* PITP A^{T64D} and *Gd* PITP B^{T64D} will be used to determine the counter ligand as they will be unable to bind to PtdIns, the preferential binding lipid. These lipids were then identified via mass spectroscopy (MS). Unfortunately, MS optimisation is still underway and has yet to enable identification of the bound lipids.

4.3 Discussion

To date, *G. duodenalis* has been identified to encode for a single, putative PITP. Although nothing is known about this protein it is hypothesised that, from gene expression analysis, *Gd* PITP is required during encystation. Cholesterol has been shown to be an important lipid during the *G. duodenalis* lifecycle [26]. As cholesterol availability diminishes, the parasite undergoes encystation to form an environmentally resistant form. In an attempt to characterise *Gd* PITP, we wanted to determine its lipid binding potential. Bioinformatic analysis suggests that it binds to PtdIns as it possessed the PtdIns binding residues conserved in PITPα, its closest homologue. Given that the critical binding residues for PtdCho are not conserved in *Gd* PITP is suggestive that *Gd* PITP binds to a different counter ligand. Given that cholesterol is an integral lipid in the lifecycle of *G. duodenalis*, we wanted to investigate the binding potential and affinity of *Gd* PITP.

Attempts to characterise the *Gd* PITP counter ligand have been unsuccessful with current methods. Currently, the non-targeted approach will require further optimisation which is most likely attributed to the difficulty of determining a lipid binding profile via MS.

Given the hypothesis that *Gd* PITP may bind to cholesterol, the targeted approach was run alongside. Results collected from this experiment are inconclusive given that there was no significant difference between each sample, including that of the negative and positive control. Previous lipid binding experiments utilising tritiated cholesterol (^{3}H) performed by Mousley et al., 2012 confirmed Kes1p o be a potent cholesterol binding protein unlike Sec14p and the sterol binding mutant *Kes1*^{Y97F} [66]. Overall, these results are suggestive of background fluorescence and not a true representation of the lipid binding activity of these proteins.

When investigating potential issues with this assay and what may be the cause of this low fluorescence, we notice the position of the NBD moiety of TopFluor® (NDB) cholesterol to be less than ideal. Initial binding to TopFluor® (NDB) cholesterol would position the fluorescent BODIPY™ 493/503 group at the opening of the binding pocket. We suggest that the NBD moiety prevents appropriate binding of the cholesterol tail to the lid of the protein, which otherwise locks the lipid in place. Therefore, the protein cannot bind to the lipid in a typical stable conformation.

Following the issues arising from this NDB cholesterol, we sort to utilise a fluorescent cholesterol that does not require a large fluorescent molecule to measure its presence. This lipid was dihydroergosterol (DHE). DHE is a naturally fluorescent 'label-free' form of ergosterol that is utilised in various lipid transfer assays measuring the exchange of lipids between a donor vesicle containing the fluorescent molecule DHE and acceptor lipid vesicle as described in [48]. Due to time constrains and availability of equipment, this assay was not able to be replicated in the context of *Gd* PITP.

Here we adapted the method used with TopFluor® cholesterol to utilise DHE as a replacement for NBD-labelled cholesterol. Unfortunately, this was unsuccessful as the fluorescence range required to measure the DHE also matches the fluorescent range of imidazole, as such the fluorescence signal provided by imidazole saturates that of DHE alone.

To compare, TopFluor® had excellent fluorescence for the experiment it was intended but not great structure in terms of binding to the proteins. On the other hand, DHE was the correct structure for binding and best represented a cholesterol molecule but unfortunately had inferior fluorescence compared to NBD cholesterol.

Therefore, in the future to determine whether *Gd* PITP binds to sterol, the DHE transfer assay performed in [48] or the tritiated cholesterol (H^3) assay would be adopted as per [48, 53].

In higher eukaryotes, the signalling and trafficking of sterols are integral. So much so that there is a specific family of proteins dedicated to this role, the steroidogenic acute regulatory protein (StAR) – related lipid transfer (StART) domain protein, also known as the StAR D proteins [67]. These proteins are characterised by their ability to signal bind and carry cholesterol to the mitochondria. These proteins contain a hemi-beta barrel or 'helix-grip' binding pocket [67]. This pocket is made of predominantly anti-parallel beta-sheets and alpha helices securing this open beta-barrel structure, similar to that of a tunnel that accommodates the hydrophilic cholesterol molecule [67].

In higher eukaryotes, both PtdIns and cholesterol are so integral in cellular function that there are two distinct families of proteins responsible for two distinct processes/functions. Given this, we hypothesise that *G. duodenalis* may also encode for a protein to complete this process given the importance of cholesterol in their lifecycle.

Bioinformatical analysis of the *G. duodenalis* through a BLASTp search of StAR D 1-6 has not revealed any obvious StAR D proteins. Given the importance of cholesterol in the lifecycle of *G. duodenalis* we find this to be interesting as no obvious StAR D protein is found. It may be possible that *Gd* PITP may be this protein and possess the function of two proteins in one. This idea of a dual-functioning protein is not outside of the protein realm as this has been seen in other parasites. For example Toxoplasma has been described to encode for a protein harbouring both PITP and Oxysterol Binding Protein (OSBP) activity [68].

Understanding the function of *Gd* PITP in the lifecycle of *G. duodenalis* has expanded the various avenues whereby the molecular mechanisms that control particular processes in the lifecycle, such as encystation can be investigated. One such avenue is though exploration into the lipid binding properties of *Gd* PITP, which due to its non-classical nature and similarity to Sfh3p, supports our hypothesis that it may be involved in the binding, transport, and exchange of sterols, specifically cholesterol. Future studies should aim to explore and optimise these avenues to further characterise *Gd* PITP and its lipid binding activity which will aid in the understanding in the process

of encystation which will in turn work towards identifying a target to mitigate the burden of infection of *G. duodenalis*.

Chapter 5

Concluding discussion

Giardia duodenalis is a common intestinal parasite responsible for causing diarrhoeal disease worldwide. It is estimated to cause 280 million symptomatic cases worldwide with those that are symptomatic experiencing unpleasant symptoms such as diarrhoea, nausea which may lead to malnutrition [1, 3, 4]. Prevalence of *G. duodenalis* infection across the world is seen between 2-5% in developed countries with infections rates as high as 20-30% in developing countries. Though Australia has a prevalence of infection aligned with developed countries, there are remote indigenous communities within Australia that experience infection rates equal to or higher than some developing countries. For example, up to 32% of children in remote communities in the north of Western Australia and up to 66% of children in remote communities in the Northern Territory infected [9, 10].

Giardia duodenalis undergoes a two-stage lifecycle, excystation which is the process where a trophozoite is liberated from the cyst, causing infection. The second stage of the lifecycle, encystation is the process, triggered through factors such as low cholesterol and high bile, that encapsulates the parasite within an environmentally resistant cyst. Following the completion of this process, the cyst can be released into the environment and be up taken by a host and allow the lifecycle to begin again. As encystation is responsible for the formation of the environmentally resistant cyst and therefore the transmission of disease was the focus of this study.

During encystation, the morphological structures of the trophozoite are internalised. In addition to this, the synthesis, packaging, and transport of CWPs via ESVs where they are exported to the cyst periphery to form the extracellular matrix forming the cyst wall. This is the only known stage-specific regulated export pathway of *G. duodenalis*. In other eukaryotes, the Golgi complex is the central component of secretion of cellular components though *G. duodenalis* interestingly lacks a rudimentary Golgi. However, it is hypothesised that ESVs are a stage-specific Golgi equivalent.

Though encystation is important for the transmission of disease, the molecular mechanisms that control encystation are poorly understood. Therefore, in order to further understand encystation, it is crucial to identify any novel regulators of this process.

A whole cell proteomic analysis of *G. duodenalis* showed the increased expression of the protein, PITP, termed *Gd* PITP, an uncharacterised protein in *G. duodenalis*. However, PITPs have been extensively investigated in other organisms such as yeast and humans. Given this, we utilised what was known about PITPs in these eukaryotes to investigate the *Gd* PITP.

PITPs can be broken down into two groups based on their activity, the 'classical' binding to PtdIns and PtdCho and the 'non-classical' that bind to PtdIns and a different counter ligand. An alignment of *Gd* PITP against its closest homologue, mammalian PITPα, a classical PITP identified that the critical residues required for PtdIns binding are conserved in *Gd* PITP. Though the critical binding residues required for PtdCho binding were not conserved suggesting that *Gd* PITP is a 'non-classical' PITP. To further investigate *Gd* PITP we investigated the critical PtdIns residues and one particular residue that was of interest was T64 (59 in PITPα) and utilised a mutant of *Gd* PITP where T64 was mutated to D. This residue was chosen due to its use in early studies into altered PtdIns binding and its ability to ablate PtdIns binding whilst maintaining a stable protein [38].

Given that we believe *Gd* PITP to be a non-classical PITP we utilised the highly characterised, classical yeast PITP, Sec14p was used. Temperature sensitive mutants of Sec14p has been used to investigate function of various PITPs and is useful due to the ability to exploit yeast due to its genetic tractability, to investigate proteins in other organisms and essentially use yeast as a 'test tube'. One way yeast can be utilised as a model is through the use of a *ts* mutant of the highly characterised Sec14p, *sec14-1ts* to investigate and characterise PITPs in other organisms. In this instance, the characterisation of *G. duodenalis*. Typically, heterologous expressing of a classical PITP in *sec14-1ts* will allow growth of these cells at 30°C, 34°C and 37°C. On the other hand, heterologous expression of a non-classical PITP will allow *sec14-1ts* to grow at 30°C, may allow growth at 34°C but will not allow growth at 37°C.

When the *Gd* PITP A and *Gd* PITP B were overexpressed in *sec14-1ts* yeast, the cells had an exacerbated growth defect. This not only didn't allow growth at 37°C which would be expected for a non-classical PITP, additionally it allowed only minor growth at 30°C. Interestingly, when the PtdIns binding mutants, *Gd* PITP^{T64D} were over expressed in these *ts* cells, the growth represented that of vector control and restored

growth to a vector control level at 30°C. When overexpressed in *pik1-101ts*, the PtdIns-4-P kinase, *Gd* PITP affected growth of these *ts* cells in the same way. Given that the PtdIns binding mutant T64D allowed growth of these ts cells at the permissive 30°C when the WT protein did not, suggests that these effects on growth are PtdIns centric.

Interestingly, this growth phenotype observed with *Gd* PITP has been observed only once previously and that is with a specific yeast PITP, Sfh3p, a homologue of Sec14p. Sec14 is a recently characterised protein though the interesting thing about Sfh3, other than the similar phenotype with *Gd* PITP is that Sfh3 is a PITP that is specifically involved in sporulation in yeast. Sporulation is a stress response in response to nutrient depletion. Though sporulation is a different process to encystation, there are parallels that can be drawn between the two processes. Given this, we found it to be more than a coincidence that Sfh3p is upregulated specifically during sporulation, when *Gd* PITP was also seen to be upregulated during encystation. Given the similarities, Sfh3p was used as a model to further investigate the function of *Gd* PITP.

When this exacerbated growth phenotype was observed in *sec14-1ts* that overexpressed Sfh3p, it was found that this exacerbated growth phenotype was due to a re-direction of essential PtdIns-4-P production from the TGN to LD preventing the breakdown of neutral lipids.

To investigate whether *Gd* PITP is affecting LD metabolism in the same way as Sfh3, fluorescent microscopy and flow cytometry was used, staining for neutral lipids with BODIPY™ 493/509. *Sec14-1ts* cells over expressing *Gd* PITP A and *Gd* PITP A^{T64D} were investigated. Results from flow cytometry and microscopy revealed results corresponding with the growth phenotype where the cells expressing *Gd* PITP A saw a larger number of cells with a larger number of fluorescently staining neutral lipids or a higher MFI compared to that of the *Gd* PITP A^{T64D} mutant. The mutant saw an MFI and a stained neutral lipid environment that was similar to that of the vector control.

Overall, *Gd* PITP has a growth phenotype and lipid droplet content within the cell reminiscent of Sfh3p. Given these results, *Gd* PITP may be a Sfh3p-like PITP involved specifically during encystation.

Furthermore, Sfh3p is characterised as being a non-classical PITP, binding to a counter ligand of sterol. Lipid binding experiments were performed with Sfh3p and tritiated cholesterol (^{3}H) and DHE. To investigate the lipid binding activity and determine whether *Gd* PITP binds to sterol or what the counter ligand of *Gd* PITP is, two experiments were performed, a targeted approach and a non-targeted approach. The non-targeted approach was performed by incubating the purified recombinant *Gd* PITP protein with whole lipid extracts from yeast. These lipids would then be identified via mass spectrometry. Optimisation is required for this experiment and the bound lipids have not been identified. For this approach, *Gd* PITP and *Gd* PITP^{T64D} will be utilised. *Gd* PITP will allow for determination of the primary lipid which we have hypothesised is PtdIns. Therefore, *Gd* PITP^{T64D} will allow for the determination of the counter ligand. We hypothesise the *Gd* PITP counter ligand is a sterol, specifically cholesterol. Given that yeast synthesise ergosterol, not cholesterol, we believe that the PtdIns binding mutant will bind to ergosterol. If we are unable to identify a counter ligand, we will then seek lipid extracts from mammalian cells. This may occur as *G. duodenalis* scavenges lipids from its host and therefore the lipids that the protein may bind to may not be present within the lipid extracts from yeast. An example is cholesterol, a lipid that has been found to be important in the life cycle of *G. duodenalis*.

Alongside the non-targeted approach, a target approach was adopted to identify the *Gd* PITP counter ligand. This experiment utilised a lipid binding experiment using TopFluor® cholesterol. Initially this lipid was utilised due to accessibility and equipment available to perform the assay. It was brought to our attention that the BODIPY™ molecule on the hydroxyl group of the cholesterol may be a limitation in this experiment and given the results seen this was an issue. Results from this assay lead to the conclusion that this large molecule attached to the cholesterol molecule inhibited the correct binding of the cholesterol molecule that was expected. This became apparent when the positive control Kes1p that has been utilised in numerous lipid binding experiments as the gold standard sterol binding control.

In an attempt to rectify this assay, the naturally fluorescent DHE was adapted to the previously developed lipid binding assay. Unfortunate different issues arose whereby the fluorescent range used allowed for the fluorescence of imidazole along with the DHE, not making it possible to distinguish the fluorescence of the DHE specifically.

Given the time availability and specialised equipment, the [^{3}H] cholesterol assay or lipid transfer assay utilising DHE as described in [48, 53] would be the preferred assay.

Given our hypothesis that *Gd* PITP may bind to a counter ligand of sterol, turned our attention to the life cycle and the importance of cholesterol. Given the importance of cholesterol in higher eukaryotes, a specific family of proteins are required for the regulated cholesterol transfer, the StAR D proteins. It is interesting that cholesterol being an integral part of the *G. duodenalis* that no StAR D proteins have been identified to date. This led to the hypothesis, given that *Gd* PITP, given its position as an early divergent eukaryote that it may be a duel functioning protein coupling the function of a PITP and StAR D protein into a single protein required during encystation. *Gd* PITP may act as a model for understanding the evolution of both PITPs and StAR D proteins in higher eukaryotes.

In addition to the characterisation of the binding activity of *Gd* PITP, we also want to investigate its role in PtdIns-4-P metabolism. In eukaryotes, PtdIns-4-P is required for the recruitment of proteins required for secretory function and trafficking from the Golgi, targeting to the plasma membrane. A puromycin selectable expression vector is currently under construction whereby its completion will allow for the promotor and ORF from the *Gd* PITP and its mutant derivatives to be GFP tagged and allow for visualisation. Here the puromycin selectable vector will be electroporated into *G. duodenalis* and these cells will be induced to undergo encystation. During encystation, fluorescent microscopy will be performed over a time course of every 15 minutes for an hour and every 3 hours up to 24 hours to capture fluorescent expression of *Gd* PITP. In addition to this, this vector will be cloned to contain one of the following PtdIns-4-P specific reporters (GFP-GOLPH3 or GFP-2xPH^{Osh2}) to detect intracellular pools of PtdIns-4-P within *G. duodenalis*.

Given the alarming infection rates across the world and specifically in some remote regions of Australia it is important to understand the lifecycle of this parasite. Specifically, the process of encystation as it is responsible for the formation of the environmentally resistant cyst. Therefore, identifying key regulators of this process may aid in for formation of a pharmaceutical target of this process to therefore block the formation of the cyst and spread of infection. This study has led to the hypothesis that *Gd* PITP may be a key regulator in encystation.

8.0 References

1. Adam RD. Biology of Giardia lamblia. Microbiol Rev. 2001;14(3):447-75. doi:10.1128/cmr.14.3.447-475.2001
2. Sogin ML, Gunderson JH, Elwood HJ, Alonso RA, Peattie DA. Phylogenetic meaning of the kingdom concept: an unusual ribosomal RNA from Giardia lamblia. Science. 1989;243(4887):75-7. doi:10.1126/science.2911720
3. Adam RD. The biology of Giardia spp. Clin Microbiol Rev. 1991;55(4):706-32.
4. Einarsson E, Svärd S. Encystation of Giardia intestinalis-a journey from the duodenum to the colon. Curr Trop Med Rep. 2015;2 doi:10.1007/s40475-015-0048-9
5. Lujan HD, Mowatt MR, Nash TE. The molecular mechanisms of giardia encystation. Parasitol Today. 1998;14(11):446-50.
6. Yichoy M, Duarte TT, De Chatterjee A, Mendez TL, Aguilera KY, Roy D, et al. Lipid metabolism in Giardia: a post-genomic perspective. Parasitology. 2011;138(3):267-78. doi:10.1017/S0031182010001277
7. Cacciò SM, Ryan U. Molecular epidemiology of giardiasis. Molecular and Biochemical Parasitology. 2008;160(2):75-80. doi:https://doi.org/10.1016/j.molbiopara.2008.04.006
8. Júlio C, Vilares A, Oleastro M, Ferreira I, Gomes S, Monteiro L, et al. Prevalence and risk factors for Giardia duodenalis infection among children: A case study in Portugal. Parasites & Vectors [journal article]. 2012;5(1):22. Júlio2012; doi:10.1186/1756-3305-5-22
9. Gracey M. Diarrhoea in Australian Aborigines. Aust J Public Health. 1992;16(3):216-25.
10. Gracey M. Gastro-enteritis in Australian children: studies on the aetiology of acute diarrhoea. Annals of Tropical Paediatrics. 1988;8(2):68-75. doi:10.1080/02724936.1988.11748542
11. Buret AG, Amat CB, Manko A, Beatty JK, Halliez MCM, Bhargava A, et al. Giardia duodenalis: New Research Developments in Pathophysiology, Pathogenesis, and Virulence Factors. Current Tropical Medicine Reports. 2015;2(3):110-118. doi:10.1007/s40475-015-0049-8

12. Morrison HG, McArthur AG, Gillin FD, Aley SB, Adam RD, Olsen GJ, et al. Genomic minimalism in the early diverging intestinal parasite Giardia lamblia. Science. 2007;317(5846):1921-6. doi:10.1126/science.1143837

13. Ryan U, Caccio SM. Zoonotic potential of Giardia. Int J Parasitol. 2013;43(12-13):943-56. doi:10.1016/j.ijpara.2013.06.001

14. Heyworth MF. Giardia duodenalis genetic assemblages and hosts. Parasite. 2016;23:13. doi:10.1051/parasite/2016013

15. Cacciò SM, Lalle M, Svärd SG. Host specificity in the Giardia duodenalis species complex. Infection, Genetics and Evolution. 2018;66:335-345. doi:https://doi.org/10.1016/j.meegid.2017.12.001

16. Einarsson E, Troell K, Hoeppner MP, Grabherr M, Ribacke U, Svärd SG. Coordinated Changes in Gene Expression Throughout Encystation of Giardia intestinalis. PLOS Neglected Tropical Diseases. 2016;10(3):e0004571. doi:10.1371/journal.pntd.0004571

17. Ankarklev J, Jerlstrom-Hultqvist J, Ringqvist E, Troell K, Svard SG. Behind the smile: cell biology and disease mechanisms of Giardia species. Nat Rev Microbiol. 2010;8(6):413-22. doi:10.1038/nrmicro2317

18. Gottig N, Elias EV, Quiroga R, Nores MJ, Solari AJ, Touz MC, et al. Active and passive mechanisms drive secretory granule biogenesis during differentiation of the intestinal parasite Giardia lamblia. J Biol Chem. 2006;281(26):18156-66. doi:10.1074/jbc.M602081200

19. Einarsson E, Troell K, Hoeppner MP, Grabherr M, Ribacke U, Svärd SG. Coordinated changes in gene expression throughout encystation of Giardia intestinalis. PLoS Negl Trop Dis. 2016;10(3):e0004571. doi:10.1371/journal.pntd.0004571

20. Gerwig GJ, van Kuik JA, Leeflang BR, Kamerling JP, Vliegenthart JF, Karr CD, et al. The Giardia intestinalis filamentous cyst wall contains a novel beta(1-3)-N-acetyl-D-galactosamine polymer: a structural and conformational study. Glycobiology. 2002;12(8):499-505.

21. Lauwaet T, Davids BJ, Reiner DS, Gillin FD. Encystation of Giardia lamblia: A model for other parasites. Current opinion in microbiology. 2007;10(6):554-559. doi:10.1016/j.mib.2007.09.011

22. Olson ME, Goh J, Phillips M, Guselle N, McAllister TA. Giardia Cyst and Cryptosporidium Oocyst Survival in Water, Soil, and Cattle Feces. Journal of

Environmental Quality. 1999;28(6):1991-1996. doi:https://doi.org/10.2134/jeq1999.00472425002800060040x

23. Monis PT, Thompson RC. Cryptosporidium and Giardia-zoonoses: fact or fiction? Infect Genet Evol. 2003;3(4):233-44.

24. Bittencourt-Silvestre J, Lemgruber L, de Souza W. Encystation process of Giardia lamblia: morphological and regulatory aspects. Arch Microbiol. 2010;192(4):259-65. doi:10.1007/s00203-010-0554-z

25. Bernander R, Palm JED, Svärd SG. Genome ploidy in different stages of the Giardia lamblia life cycle. Cellular Microbiology. 2001;3(1):55-62. doi:10.1046/j.1462-5822.2001.00094.x

26. Lujan HD, Mowatt MR, Byrd LG, Nash TE. Cholesterol starvation induces differentiation of the intestinal parasite Giardia lamblia. Proc Natl Acad Sci U S A. 1996;93(15):7628-33. Available from: http://www.ncbi.nlm.nih.gov/pubmed/8755526

27. Luján HD, Mowatt MR, Nash TE. Mechanisms of Giardia lamblia differentiation into cysts. Microbiology and molecular biology reviews : MMBR. 1997;61(3):294-304. Available from: https://www.ncbi.nlm.nih.gov/pubmed/9293183

https://www.ncbi.nlm.nih.gov/pmc/articles/PMC232612/

28. Lujan HD, Mowatt MR, Conrad JT, Bowers B, Nash TE. Identification of a novel Giardia lamblia cyst wall protein with leucine-rich repeats. Implications for secretory granule formation and protein assembly into the cyst wall. J Biol Chem. 1995;270(49):29307-13. doi:10.1074/jbc.270.49.29307

29. McDermott MI, Mousley CJ. Lipid transfer proteins and the tuning of compartmental identity in the Golgi apparatus. Chem Phys Lipids. 2016;200:42-61. doi:10.1016/j.chemphyslip.2016.06.005

30. Bankaitis VA, Aitken JR, Cleves AE, Dowhan W. An essential role for a phospholipid transfer protein in yeast Golgi function. Nature. 1990;347(6293):561-2. doi:10.1038/347561a0

31. Jackson CL, Walch L, Verbavatz JM. Lipids and Their Trafficking: An Integral Part of Cellular Organization. Dev Cell. 2016;39(2):139-153. doi:10.1016/j.devcel.2016.09.030

32. Grabon A, Bankaitis VA, McDermott MI. The Interface Between Phosphatidylinositol Transfer Protein Function and Phosphoinositide Signaling in Higher Eukaryotes. Journal of Lipid Research. 2018 doi:10.1194/jlr.R089730

33. Majerus PW, York JD. Phosphoinositide phosphatases and disease. Journal of Lipid Research. 2009;50(Supplement):S249-S254. doi:10.1194/jlr.R800072-JLR200

34. Bankaitis VA, Malehorn DE, Emr SD, Greene R. The Saccharomyces cerevisiae SEC14 gene encodes a cytosolic factor that is required for transport of secretory proteins from the yeast Golgi complex. J Cell Biol. 1989;108(4):1271-81. Available from: http://www.ncbi.nlm.nih.gov/pubmed/2466847

35. Bankaitis VA, Phillips S, Yanagisawa L, Li X, Routt S, Xie Z. Phosphatidylinositol transfer protein function in the yeast Saccharomyces cerevisiae. Adv Enzyme Regul. 2005;45:155-70. doi:10.1016/j.advenzreg.2005.02.014

36. Cockcroft S. The diverse functions of phosphatidylinositol transfer proteins. Curr Top Microbiol Immunol. 2012;362:185-208. doi:10.1007/978-94-007-5025-8_9

37. Cockcroft S. Phosphatidylinositol transfer proteins: a requirement in signal transduction and vesicle traffic. Bioessays. 1998;20(5):423-32. doi:10.1002/(sici)1521-1878(199805)20:5<423::aid-bies9>3.0.co;2-o

38. Cockcroft S, Carvou N. Biochemical and biological functions of class I phosphatidylinositol transfer proteins. Biochim Biophys Acta. 2007;1771(6):677-91. doi:10.1016/j.bbalip.2007.03.009

39. Wiedemann C, Cockcroft S. The Role of Phosphatidylinositol Transfer Proteins (PITPs) in Intracellular Signalling. Trends Endocrinol Metab. 1998;9(8):324-8. doi:10.1016/s1043-2760(98)00080-0

40. Hsuan J, Cockcroft S. The PITP family of phosphatidylinositol transfer proteins. Genome biology. 2001;2(9):REVIEWS3011-REVIEWS3011. doi:10.1186/gb-2001-2-9-reviews3011

41. Cockcroft S. Chapter 142 - Phosphatidylinositol Transfer Proteins. In: Bradshaw RA, Dennis EA, editors. Handbook of Cell Signaling (Second Edition). San Diego: Academic Press; 2010. p. 1151-1158.

42. Bankaitis VA, Aitken JR, Cleves AE, Dowhan W. An essential role for a phospholipid transfer protein in yeast Golgi function. Nature. 1990;347(6293):561-562. doi:10.1038/347561a0

43. Grabon A, Khan D, Bankaitis VA. Phosphatidylinositol transfer proteins and instructive regulation of lipid kinase biology. Biochim Biophys Acta. 2015;1851(6):724-35. doi:10.1016/j.bbalip.2014.12.011

44. Cockcroft S. Phosphatidylinositol transfer proteins couple lipid transport to phosphoinositide synthesis. Semin Cell Dev Biol. 2001;12(2):183-91. doi:10.1006/scdb.2000.0235

45. Grabon A, Orlowski A, Tripathi A, Vuorio J, Javanainen M, Rog T, et al. Dynamics and energetics of the mammalian phosphatidylinositol transfer protein phospholipid exchange cycle. J Biol Chem. 2017;292(35):14438-14455. doi:10.1074/jbc.M117.791467

46. Ren J, Pei-Chen Lin C, Pathak MC, Temple BRS, Nile AH, Mousley CJ, et al. A phosphatidylinositol transfer protein integrates phosphoinositide signaling with lipid droplet metabolism to regulate a developmental program of nutrient stress–induced membrane biogenesis. Mol Biol Cell. 2014;25(5):712-727. doi:10.1091/mbc.E13-11-0634

47. Nile AH, Tripathi A, Yuan P, Mousley CJ, Suresh S, Wallace IM, et al. PITPs as targets for selectively interfering with phosphoinositide signaling in cells. Nat Chem Biol. 2014;10(1):76-84. doi:10.1038/nchembio.1389

48. Tripathi A, Martinez E, Obaidullah AJ, Lete MG, Lönnfors M, Khan D, et al. Functional Diversification of the Chemical Landscapes of Yeast Sec14-like Phosphatidylinositol Transfer Protein Lipid-Binding Cavities. Journal of Biological Chemistry. 2019 doi:10.1074/jbc.RA119.011153

49. Cockcroft S. Trafficking of phosphatidylinositol by phosphatidylinositol transfer proteins. Biochem Soc Symp. 2007 (74):259-71. doi:10.1042/bss0740259

50. Li X, Routt SM, Xie Z, Cui X, Fang M, Kearns MA, et al. Identification of a novel family of nonclassic yeast phosphatidylinositol transfer proteins whose function modulates phospholipase D activity and Sec14p-independent cell growth. Mol Biol Cell. 2000;11(6):1989-2005. doi:10.1091/mbc.11.6.1989

51. Routt SM, Ryan MM, Tyeryar K, Rizzieri KE, Mousley C, Roumanie O, et al. Nonclassical PITPs activate PLD via the Stt4p PtdIns-4-kinase and modulate function of late stages of exocytosis in vegetative yeast. Traffic. 2005;6(12):1157-72. doi:10.1111/j.1600-0854.2005.00350.x

52. Mousley CJ, Tyeryar KR, Vincent-Pope P, Bankaitis VA. The Sec14-superfamily and the regulatory interface between phospholipid metabolism and membrane

trafficking. Biochimica et biophysica acta. 2007;1771(6):727-736. doi:10.1016/j.bbalip.2007.04.002

53. Ren J, Pei-Chen Lin C, Pathak M, R S Temple B, H Nile A, Mousley C, et al. A phosphatidylinositol transfer protein integrates phosphoinositide signaling with lipid droplet metabolism to regulate a developmental program of nutrient stress-induced membrane biogenesis. 2014.

54. Bankaitis VA, Vincent P, Merkulova M, Tyeryar K, Liu Y. Phosphatidylinositol transfer proteins and functional specification of lipid signaling pools. Advances in enzyme regulation. 2007;47:27-40. doi:10.1016/j.advenzreg.2006.12.007

55. Nile AH, Bankaitis VA, Grabon A. Mammalian diseases of phosphatidylinositol transfer proteins and their homologs. Clinical lipidology. 2010;5(6):867-897. doi:10.2217/clp.10.67

56. Qiu B, Simon MC. BODIPY 493/503 staining of neutral lipid droplets for microscopy and quantification by flow cytometry. Bio-protocol. 2016;6(17) doi:10.21769/BioProtoc.1912

57. Hehl AB, Marti M. Secretory protein trafficking in Giardia intestinalis. Mol Microbiol. 2004;53(1):19-28. doi:10.1111/j.1365-2958.2004.04115.x

58. Touz MC, Zamponi N. Sorting without a Golgi complex. Traffic. 2017;18(10):637-645. doi:10.1111/tra.12500

59. Wyckoff GJ, Solidar A, Yoden MD. Phosphatidylinositol transfer proteins: sequence motifs in structural and evolutionary analyses. J Biomed Sci Eng. 2010;3(1):65-77. doi:10.4236/jbise.2010.31010

60. Bankaitis VA, Mousley CJ, Schaaf G. The Sec14 superfamily and mechanisms for crosstalk between lipid metabolism and lipid signaling. Trends Biochem Sci. 2010;35(3):150-60. doi:10.1016/j.tibs.2009.10.008

61. Mousley CJ, Tyeryar KR, Ryan MM, Bankaitis VA. Sec14p-like proteins regulate phosphoinositide homoeostasis and intracellular protein and lipid trafficking in yeast. Biochem Soc Trans. 2006;34(Pt 3):346-50. doi:10.1042/bst0340346

62. Neiman AM. Sporulation in the budding yeast saccharomyces cerevisiae. Genetics. 2011;189(3):737-765. doi:10.1534/genetics.111.127126

63. Grabon A, Bankaitis VA, McDermott MI. The interface between phosphatidylinositol transfer protein function and phosphoinositide signaling in higher eukaryotes. Journal of Lipid Research. 2019;60(2):242-268. doi:10.1194/jlr.R089730

64. Graham TR, Burd CG. Coordination of Golgi functions by phosphatidylinositol 4-kinases. Trends Cell Biol. 2011;21(2):113-21. doi:10.1016/j.tcb.2010.10.002

65. Schaaf G, Ortlund EA, Tyeryar KR, Mousley CJ, Ile KE, Garrett TA, et al. Functional anatomy of phospholipid binding and regulation of phosphoinositide homeostasis by proteins of the sec14 superfamily. Mol Cell. 2008;29(2):191-206. doi:10.1016/j.molcel.2007.11.026

66. Mousley CJ, Yuan P, Gaur NA, Trettin KD, Nile AH, Deminoff SJ, et al. A sterol-binding protein integrates endosomal lipid metabolism with TOR signaling and nitrogen sensing. Cell. 2012;148(4):702-15. doi:10.1016/j.cell.2011.12.026

67. Alpy F, Tomasetto C. Give lipids a START: the StAR-related lipid transfer (START) domain in mammals. Journal of Cell Science. 2005;118(13):2791-2801. doi:10.1242/jcs.02485

68. Graboń A. Atomistic and Cellular Analysis of Start Phosphatidylinositol Transfer Proteins in the Context of the Phospholipid Extraction Mechanism and Phosphoinositide Signaling in the Parasite Toxoplasma. 2016 doi:https://doi.org/10.17615/r2qv-v690

69. Lamming C. Expression and Packaging Mechanisms of Cyst Wall Proteins in Encysting Giardia: Curtin University; 2017

6.0 Appendices

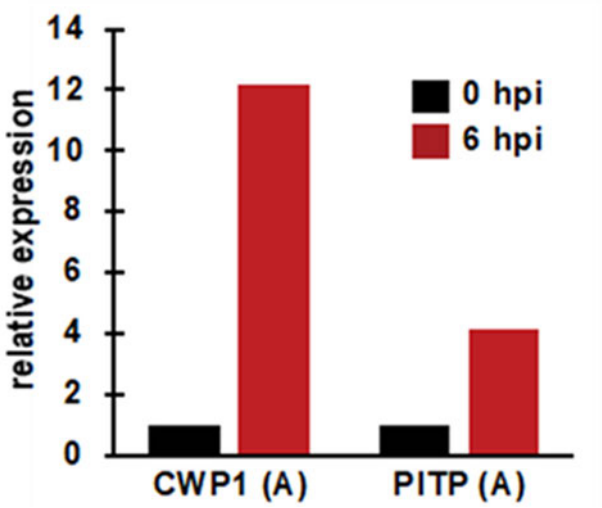

Figure S1. Expression of *Gd* PITP A at 0 and 6 h.p.i relative to CWP1 A [69]

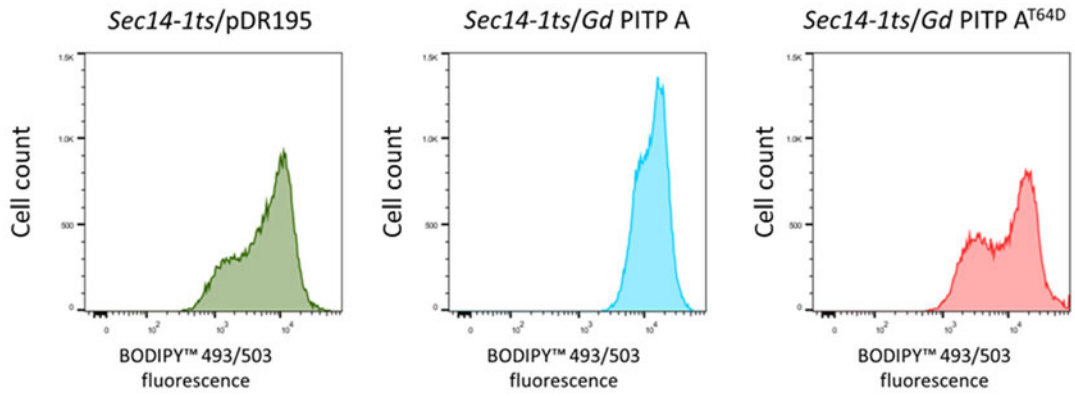

Sample	Singlets Median BODIPY™ 493/503 Total singlet count: 47625	Sample	Singlets Median BODIPY™ 493/503 Total singlet count: 47636	Sample	Singlets Median BODIPY™ 493/503 Total singlet count: 47720
Sec14-1ts/pDR195 unstained	155	*Sec14-1ts/Gd* PITP A unstained	1783	*Sec14-1ts/Gd* PITP A^{T64D} unstained	204
Sec14-1ts/pDR195 BODIPY™ 493/503	6582	*Sec14-1ts/Gd* PITP A BODIPY™ 493/503	13285	*Sec14-1ts/Gd* PITP A^{T64D} BODIPY™ 493/503	10421

Figure S2. Fluorescence intensity of *sec14-1ts* cells overexpressing pDR195, *Gd* PITP A and *Gd* PITP A^{T64D} accompanied with table of cell count of singlets and median fluorescence intensity of unstained and BODIPY^{TM} 493/503 cells.